Received: 8 November 2023 | Revised: 15 April 2024 | Accepted: 22 May 2024

DOI: 10.1002/jex2.161

RESEARCH ARTICLE

Characterisation of sRNAs enriched in outer membrane vesicles of pathogenic *Flavobacterium psychrophilum* causing Bacterial Cold Water Disease in rainbow trout

Pratima Chapagain[1] | **Ali Ali**[2] | **Destaalem T. Kidane**[3] | **Mary Farone**[3] | **Mohamed Salem**[2]

[1]Department of Medicine, Division of Diabetes, Endocrinology and Metabolism, Vanderbilt University Medical Center, Nashville, Tennessee, USA

[2]Department of Animal and Avian Sciences, University of Maryland, College Park, Maryland, USA

[3]Department of Biology and Molecular Bioscience Program, Middle Tennessee State University, Murfreesboro, Tennessee, USA

Correspondence
Mohamed Salem, Department of Animal and Avian Sciences, University of Maryland, College Park, Maryland, USA. Email: mosalem@umd.edu

Abstract

Flavobacterium psychrophilum (*Fp*) causes Bacterial Cold Water Disease in salmonids. During host-pathogen interactions, gram-negative bacteria, such as *Fp*, release external membrane vesicles (OMVs) harbouring cargos, such as DNA, RNA and virulence factors. This study aimed to characterise the potential role of the OMVs' small RNAs (sRNAs) in the *Fp*-rainbow trout host-pathogen interactions. sRNAs carried within OMVs were isolated from *Fp*. RNA-Seq datasets from whole-cell *Fp* and their isolated OMVs indicated substantial enrichment of specific sRNAs in the OMVs compared to the parent cell. Many of the OMV-packaged sRNAs were located in the pathogenicity islands of *Fp*. Conservation of sRNAs in 65 strains with variable degrees of virulence was reported. Dual RNA-Seq of host and pathogen transcriptomes on day 5 post-infection of *Fp* -resistant and -susceptible rainbow trout genetic lines revealed correlated expression of OMV-packaged sRNAs and their predicted host's immune gene targets. In vitro, treatment of the rainbow trout epithelial cell line RTgill-W1 with OMVs showed signs of cytotoxicity accompanied by dynamic changes in the expression of host genes when profiled 24 h following treatment. The OMV-treated cells, similar to the *Fp* -resistant fish, showed downregulated expression of the suppressor of cytokine signalling 1 (SOCS1) gene, suggesting induction of phagosomal maturation. Other signs of modulating the host gene expression following OMV-treatment include favouring elements from the phagocytic, endocytic and antigen presentation pathways in addition to HSP70, HSP90 and cochaperone proteins, which provide evidence for a potential role of OMVs in boosting the host immune response. In conclusion, the study identified novel microbial targets and inherent characteristics of OMVs that could open up new avenues of treatment and prevention of fish infections.

KEYWORDS
disease resistance, fish, OMVs, small RNAs

Pratima Chapagain and Ali Ali equally contributed to this work.

1 | INTRODUCTION

Flavobacterium psychrophilum (*Fp*) causes Bacterial cold-water disease (BCWD), a severe infection that frequently affects salmonid species, including salmon and rainbow trout. BCWD is responsible for causing a considerable economic loss in freshwater aquaculture of salmonids (Nematollahi et al., 2003). Losses from this infection have been reported in many countries, including the United States, the United Kingdom, Australia and Japan (Starliper, 2011). Mortality rates from this disease vary, but rates as high as 90% have been reported (Barnes & Brown, 2011). *Fp* is a psychrophilic, gram-negative bacterium typically found in cold freshwater (Madetoja. et al., 2001). After entering the host, likely through skin abrasions, *Fp* spreads through the dermis, connective and muscle tissues (Nematollahi et al., 2003). Rainbow trout (especially fry) infected by *Fp* exhibit irregular swimming behaviour, exophthalmia, darkened coloration, skeletal deformities and visible deep necrotic lesions around the caudal peduncle (Barnes & Brown, 2011). The survivability of this pathogen under various environmental conditions and the unavailability of vaccines contribute to the severity of the disease (Gomez et al., 2014).

Recent approaches have correlated fish genetic variations to immune responsiveness and survival rates after challenges with Fp (Barbier et al., 2020, Marancik et al., 2014, Wiens et al., 2013). Efforts have been made to create BCWD-resistant strains of rainbow trout. Through a selective breeding program, the National Center for Cool and Cold-Water Aquaculture (NCCCWA) developed three genetic lines of rainbow trout: BCWD-susceptible, -control and -resistant lines (Marancik et al., 2014, Wiens et al., 2013). The susceptible line has a very low survival rate (29.4%), the control line has an intermediate survival rate (54.6%) and the resistant line has undergone multiple generations of selection against *Fp* challenge to enhance their survival rate up to 94% (Marancik et al., 2014).

The molecular pathogenesis of *Fp* is still not yet completely understood. Many factors, including biofilm formation, secretion systems and virulence factors such as exotoxins, proteases and adhesins, are thought to play a role in the pathogenesis of this bacterium (Barbier et al., 2020, Nematollahi et al., 2003). *Fp*, similar to other gram-negative bacteria, produce small (<300 nm in diameter) spherical particles derived from the bacterial outer membrane, commonly known as outer membrane vesicles (OMVs) (Moller et al., 2005). Many pathogenic bacteria rely on OMVs to deliver virulence factors to their host (Ellis & Kuehn, 2010, Oliver et al., 2016), and OMV-mediated delivery has been considered an essential mechanism in host-pathogen interactions. For example, OMVs of *Porphyromonas gingivalis* contain a group of proteases, constituting the virulence factor 'gingipains', which degrade cytokines and ultimately downregulate the immune response of host cells (Haurat et al., 2011). Similarly, different cargos, such as DNA, RNA and cytosolic proteins within OMVs, can be transported to the host cell when OMVs fuse with host cell membranes or bind to the host cell receptors (Jan, 2017, Koeppen et al., 2016, van der Pol et al., 2015). sRNAs within OMVs of *Pseudomonas aeruginosa* have been shown to reduce the host immune response (Koeppen et al., 2016). We recently showed the potential role of the coding genes of *Fp*-OMVs in the host–pathogen interactions (Chapagain et al., 2023); however, the sRNAs role is yet to be explored.

Bacterial sRNAs are non-protein-coding molecules with a length typically ranging from 50 to 500 nucleotides and have essential roles in post-transcriptional gene regulation (Chao et al., 2012, Dutcher & Raghavan, 2018). sRNAs usually originate from the untranslated regions of the bacterial genome but can also be acquired by horizontal gene transfer (Dutcher & Raghavan, 2018, Padalon-Brauch et al., 2008). Many sRNAs act as complementary antisense sequences to mRNAs (Gottesman & Storz, 2011), and their function resembles eukaryotic microRNAs (miRNAs). They cause translational repression by directly hybridising with mRNAs to promote transcript degradation (Wang et al., 2015). These molecular mechanisms enable sRNAs to play a role in bacterial pathogenicity. For example, previous studies have suggested that the network of bacterial genes in biofilm formation is controlled by sRNAs (Chen et al., 2018, Kang et al., 2015). A recent study in *P. aeruginosa* has shown the involvement of sRNAs in repressing the translation of genes involved in quorum sensing by binding to the ribosome binding sites of mRNA targets (Chen et al., 2019). A study on *Staphylococcus aureus* reported the participation of sRNAs in regulating cellular responses to signal molecules (Mader et al., 2016). Another study reported that entry of bacterial sRNAs inside host cells triggers a host gene-bacterial sRNAs interaction resulting in the degradation of host immune genes (Papenfort & Bassler, 2016).

In this study, OMVs were isolated from *Fp* (strain CSF-259-93) broth culture on day 8 of bacterial growth. The parent bacteria and OMVs were subjected to RNA sequencing, and then the transcriptomic data were used for sRNAs prediction. We identified specific and/or enriched sRNAs in OMVs by comparing sRNA expression levels in the parent cells versus OMVs. Many of the OMV-packaged sRNAs were located in the pathogenicity islands of *Fp*. Sequence conservation of sRNAs was compared in 65 strains with variable degrees of virulence.

Further, dual RNA-Seq of host and pathogen revealed that bacterial sRNAs were reciprocally expressed with their in silico predicted target immune genes on day 5 following infection of selectively bred resistant- and susceptible-line rainbow trout. We also used RNA-Seq to in vitro investigate the transcriptomic effect of OMVs treatment on RTgill-W1 host cells. We noticed a similar downregulated expression of SOCS1 in *Fp*-infected resistant fish and OMV-treated cells, which could explain the high bacterial load in susceptible fish following infection. sRNAs targeting and reciprocally correlated in expression with the SOCS1 were identified. Signs of cytotoxicity were noticed; however, immune response genes expression was boosted at the early phase of OMV treatment (24 h post-treatment).

2 | MATERIALS AND METHODS

2.1 | Ethic statement

Fish were maintained at the NCCCWA, and animal experimental protocols were approved by the NCCCWA Institutional Animal Care and Use Committee Protocols #053 and #076.

2.2 | Bacterial culture

Fp (CSF 259–93) were obtained from USDA/NCCCWA (Dr. Gregory Wiens). *Fp* were cultured as we previously described (Chapagain et al., 2023). In brief, frozen stock cultures of *Fp* were cultured on Tryptone Yeast Extracts (TYEs) agar, and the plate was incubated at 15°C for 1 week. *Fp* colonies isolated from the TYEs agar plate were transferred to TYEs broth, and absorbance (525nm wavelength) was measured after 24 h of incubation. Absorbance was measured every day for 2 weeks to determine the log phase of the cultures. TYEs broth culture without *Fp* was used as a negative control.

2.3 | Isolation of OMVs

OMVs were isolated from *Fp* broth culture on day 8 of bacterial growth as we previously described (Chapagain et al., 2023). In brief, a loopful of culture was sub-cultured onto a plate on day 7 of bacterial growth to ensure the broth was free of contamination. For OMV isolation, broth culture from a flask was distributed into several 50 mL tubes. Each tube was centrifuged at 2800 × *g* for 1 h at 4°C to pellet the bacterial cells. To remove any remaining bacterial cells, the supernatant was collected and filtered through a 250 mL sterile 0.22 μm PES membrane filter (EMD Millipore Corporation, Billerica, MA, USA). The filtrate was then subjected to ultracentrifugation for 3 h at 40,000 rpm and 4°C to pellet the OMVs. The OMV pellet was washed with phosphate-buffered saline (PBS) and again subjected to ultracentrifugation for 2 h at 40,000 rpm and 4°C to re-pellet the OMVs. The OMV pellet was resuspended in nuclease-free water and stored at −20°C. To ensure that the suspension containing OMVs was free of bacteria, 30 μL of the suspension was cultured on a TYEs agar plate and incubated for 10 days. After 10 days, no bacterial growth was observed in TYEs agar.

2.4 | Nanoparticle tracking analysis (NTA)

Nanoparticle tracking analysis (NTA), using ZetaView (Particle Metrix, Germany), was conducted to measure the size and concentration of OMVs isolated from *Fp*. The instrument settings included a laser wavelength of 488 nm, filter wavelength set to Scatter, sensitivity at 85.0 and Shutter at 100. The videos were analysed using the built-in ZetaView Software (version 8.05.16 SP7). Analysis parameters were configured with a maximum area of 1000, minimum area of 0, minimum brightness of 65 and nm/class set to 10.

2.5 | Bacterial RNA extraction, cDNA library preparation and sequencing

RNA extraction and downstream processing for sequencing were previously described (Chapagain et al., 2023). Briefly, RNA was extracted from *Fp* colonies isolated from a TYEs agar plate and from OMVs isolated from *Fp* broth culture using TriZol reagent (Invitrogen, Carlsbad, CA, USA). The RNA concentration was measured using a Nanodrop™ ND-1000 spectrophotometer (Thermo Fisher Scientific, Waltham, MA, USA). To confirm the existence of RNA in OMVs, 4 μL of the RNA samples (∼ 500.2 ng/ μL) were treated with 2 μg/μL of RNase Cocktail Enzyme mix (Thermo Fisher Scientific, Waltham, MA, USA) and incubated in a water bath at 37°C for 30 min. RNase-treated and -untreated OMV RNA samples were then run on an agarose gel. RNA samples isolated from *Fp* and OMVs were stored at -80°C until further processing.

For library preparation and RNA sequencing, RNA samples isolated from *Fp* cells and OMVs were sent to BGI Genomics (Cambridge, MA, USA). Library preparation was performed using a Trio RNA-Seq kit (NuGEN, San Carlos, CA, USA) according to manufacturer recommendations. Briefly, rRNA was depleted and RNAs were fragmented using a fragmentation buffer. Fragmented pieces were then purified using a QiaQuick PCR extraction kit (QIAGEN, Germantown, MD, USA), and the solution was resuspended in EB buffer, and cDNA was subjected to end repair and poly (A) tail addition. The fragments were then connected with the adaptors. The library was then purified using a MinElute PCR Purification kit before PCR amplification. PCR was used to amplify the libraries, and then the yield was quantified. Sequencing was performed on an Illumina MiSeq platform

(Illumina, Inc., San Diego, CA, USA). Raw RNA-Req reads were submitted to the NCBI Short Read Archive under BioProject ID PRJNA259860 (accession number SUB10837562).

2.6 | Prediction of sRNAs and their target genes

Raw sequence reads were trimmed by removing adaptor sequences and 5 bp from each end using the CLC Genomics Workbench in accordance with the manufacturer's instructions manual followed by filtering out low-quality reads. RiboDetector software was used to assess rRNA reads depletion. The average proportion of rRNA per sample was approximately 0.02% confirming a successful rRNA depletion (Deng et al., 2022). High-quality reads from *Fp* (60,352,578 reads) and OMVs (55,722,742 reads) were used for downstream analyses. Reads from the *Fp* transcriptome and OMVs were mapped to the *Fp* (CSF-259-93) reference genome using TopHat2 (Kim et al., 2013). The FlaiMapper tool (Hoogstrate et al., 2015) was used to identify potential sRNAs. sRNAs were predicted and filtered according to their length. sRNAs greater than 500 nt long were filtered out. Further, Pred^{sRNA} (Kumar et al., 2021) was downloaded from the PresRAT webserver (http://www.hpppi.iicb.res.in/presrat) to confirm results obtained from FlaiMapper and identify high-confidence list of sRNAs. *Pred^{sRNA}* predicts novel sRNA sequences by using secondary structural information to calculate a combined score ($sRNA_{score}$). Log Odds (LOD) ratio matrices is used to calculate $Sequence_{score}$ for the input sequence. U-richness score reflects the presence of uracil at the 3′ end of the sRNA. PresRAT uses the secondary structure information to calculate a set of local minima conformations of the input sRNA sequence, then estimating the Average Base Energy (ABE_{score}) and Average Loop Energy (ALE_{score}.) of local minima secondary structure conformations. The combined score ($sRNA_{score}$,) can be calculated as follows:

$$\mathrm{sRNA_{score}} = (\mathrm{Sequence_{score}} + \mathrm{Urich_{score}} - \mathrm{ABE_{score}} - \mathrm{ALE_{score}})$$

The combined $\mathrm{sRNA_{score}}$ was used as the final scoring scheme to predict the most likely true positive sRNA from the list of sRNA instances predicted by FlaiMapper.

DE transcripts and trout immune-related genes targeted by the DE sRNAs were predicted using a locally installed LncTar software (Li et al., 2015) and IntaRNA (version 2.0) (Mann et al., 2017). A normalised deltaG (ndG) of −0.10 was used as a cutoff value to determine the potential interaction among paired RNAs.

2.7 | BCWD-resistant and -susceptible fish population and bacterial challenge

The current study used samples from two rainbow trout genetic lines of divergent resistance to BCWD. USDA-NCCCWA produced these genetic lines via a family-based selection method as previously described (Silverstein et al., 2009). Briefly, single-sire × single-dam matings were made between 3-year-old dams and 1-year-old sires (neo-males) within the genetic lines. The resistant line eggs were produced from dams that had undergone three generations of BCWD selection, whereas the sires had undergone four generations of selection to increase the disease resistance phenotype. On the other hand, the susceptible line eggs were produced from parents that had undergone one generation of selection to increase susceptibility to infection. The resistant and susceptible genetic lines had significant differences in susceptibility to *Fp* (Marancik et al., 2014, Paneru et al., 2016).

For this study, fish from resistant and susceptible genetic lines (49 days post-hatch) were challenged with *Fp* as we previously described (Marancik et al., 2014). Briefly, fifty fish were randomly assigned to each tank with 2.4 L min−1 of 12.5 ± 0.1°C flow-through spring water supply. For each genetic line, two fish tanks were intraperitoneally injected with 4.2 × 106 CFU fish−1 *Fp* suspended in 10 µL PBS, and survival was monitored daily for 21 days. Five individuals were sampled from each tank on day 5 post-injection. All fish were certified to be infection-free before being injected with *F. psychrophilum*.

2.8 | RNA sequencing and gene expression analysis of BCWD-resistant and -susceptible fish

As explained above, tissue samples used in this study were obtained from USDA/NCCCWA (Dr. Gregory D Wiens). RNA was extracted from the whole fish using TriZol (Invitrogen, Carlsbad, CA, USA), followed by quantity and quality assessments as described above. RNA samples were then treated with DNAase I (Fisher BioReagents, Hudson, NH, USA) to remove DNA from samples. For sequencing, equal amounts of RNA samples were pooled from 2 fish, and 4 pooled samples were sequenced from each of the resistant and susceptible genetic lines (i.e., a total of 8 libraries). Sequencing was done at RealSeq Biosciences, Inc. (Santa Cruz, CA, USA). The Zymo Ribofree library prep kit (Irvine, CA, USA) targeted all RNAs during the library preparation, including trout and bacterial RNAs.

The raw sequence reads from each genetic line were trimmed using the CLC Genomics Workbench in accordance with the manufacturer's instructions manual in order to obtain high-quality reads. Read mapping and gene expression analyses were performed using a CLC Genomics Workbench. Reads were separately mapped to the rainbow trout genome [USDA OmykA_1.1 assembly (GCF_013265735.2)] and *Fp* reference genomes to identify DE transcripts. Mapping criteria were as follows: mismatch cost = 2, insertion/deletion cost = 3, minimum length fraction = 0.9 and similarity fraction = 0.9. The expression value of each transcript was calculated in terms of TPM and DE transcripts between resistant and susceptible genetic lines were identified using EDGE test (FDR value < 0.05, log2 fold change cutoff ±1). Raw RNA-Req reads were submitted to the NCBI Short Read Archive under BioProject ID PRJNA259860 (accession number SUB10837562).

2.9 | Maintenance of RTgill-W1 cell line

Frozen RTgill-W1(CRL-2523) cells were obtained from ATCC (American Type Culture Collection, Manassas, VA, USA). Cells were handled according to instructions provided by ATCC. Briefly, frozen cells were thawed at 20°C in a water bath, and the full content from the vial was transferred to L-15 media (Thermo Fisher Scientific, Waltham, MA, USA) supplemented with 10% complement inactivated foetal bovine serum (FBS) and 100 units/mL of penicillin and 100 µg/mL of streptomycin (complete medium). Cells were centrifuged at 125 × *g* for 8 min, the supernatant was removed, and the cells were resuspended in a complete medium. The cells were maintained in 25 cm^2 flasks at 18°C. Media were renewed every 4 days, and cells were passaged every 8 days. Since cells are adherent, cells were dislodged by trypsinisation whilst passaging.

2.10 | Exposure of RTgill-W1 cells to OMVs

Approximately 1.2×10^6 RTgill-W1 cells/well in L-15 media supplemented with 2% FBS (Semple et al., 2020) were seeded in 6-well tissue culture plates. Before treatment, cells were maintained overnight at 18°C. A 100 µL volume of OMVs (at concentration of 7.1E+7 particles/μL) was added to cells for 6, 12 and 24 h. For control, nuclease-free water was added to cells. Each condition was run in triplicate. Plates were incubated at 18°C, and sampling was done after each incubation period. All the media from the 'control' and 'treated cells' were removed, and cells were then washed twice with PBS. The cells were trypsinised and then lysed with Trizol reagent for RNA extraction, followed by sequencing and gene expression analyses. To determine the cell viability, we performed a PrestoBlue Assay in which ~500,000 cells/well were seeded in a 96-well plate for 24 h. Cells were then treated with OMVs for different time intervals of 0 min, 6, 12 and 24 h. Each condition was run in triplicate. Nuclease-free water was added to cells as a control, and only cell culture medium was used as a blank for the PrestoBlue Assay. After treatment, PrestoBlue reagent was added to wells, and then the plate was incubated at 37°C for 10 min, followed by incubation at 18°C for 1 h. The absorbance of treated cells and controls was then measured at 570 nm wavelength to determine cell viability.

2.11 | Gene expression analyses by qPCR

For qPCR analyses, cDNA was prepared from total RNA using Verso cDNA Synthesis Kit (Thermo Fisher Scientific, Waltham, MA, USA). Each qPCR reaction contained 3 µL template (100 ng/μL), 1 µL (10 µM) forward and reverse primers, 5 µL SYBR Green Master Mix (Bio-Rad, Hercules, CA, USA) and 1 µL nuclease-free water. A negative control (same reaction but without a template) was used to ensure the samples were free of DNA contamination. β-actin (NCBI GenBank Accession number: AJ438158) and Prolyl tRNA synthetase (Hesami et al., 2011) were used as reference genes to normalise gene expression for rainbow trout genes and *Fp*, respectively. The amplification conditions were 95°C for 3 min, followed by 39 cycles. Each cycle started with 95C for 30 s, followed by a primer annealing step for 30 s, and was completed at 60°C for 30 s. An extension step at 72°C for 5 min was added. The delta-delta (ΔΔCt) method was used to quantify the gene expression and the fold change was computed using the formula $2^{-\Delta\Delta Ct}$ at a significant p-value < 0.05 (Ali et al., 2018, Paneru et al., 2018, Schmittgen & Livak, 2008).

2.12 | sRNAs conservation and identification of sRNAs within pathogenicity islands

To determine the conservation of sRNAs, DE sRNAs reported in this study were blasted against the genome sequences of 65 different *Fp* strains downloaded from the National Center for Biotechnology Information (NCBI) GenBank database (https://www.ncbi.nlm.nih.gov/genome/browse/#!/prokaryotes/1589/). *Fp* strains used in this study were 950106-1/1, DSM 3660, 010418-2/1, 4, 10, 11754, 17830, 160401-1/5, 990512-1/2A, CH8, CH1895, CHN6, CN, CR, F164, FI055, FI070, *FP* G3, *FP* G48, *FP* RT1, *FP* G1, *FP* S-F15, 160401-1/5N, P30-2B/09, F164, *FP* S-F16, *FP* S-S11A, 990512-1/2A, P15-8B/11, 160401-1/5M, *FP* S-F27, *FP* S-R7, *FP* S-S9, JIP02-86, *FP* S-S6, OSU THCO2-90, *FP* S-P3, *FP* S-P1, V46, JIP 08/99, JIP 16/00, *FP* S-S10, 010418-2/1, K9/00, 950106-1/1,

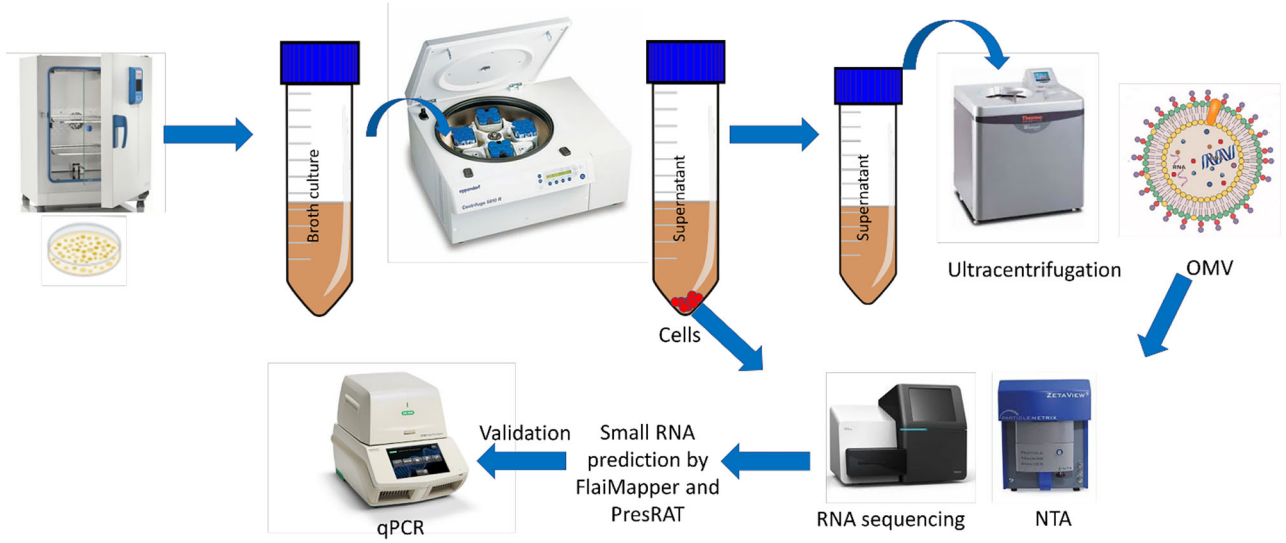

FIGURE 1 Overview of the experimental design to predict and validate bacterial small RNAs. Frozen stock cultures of *Fp* were cultured on TYEs agar, and the plate was incubated at 15°C for 1 week. *Fp* colonies isolated from TYEs agar plate were transferred to TYEs broth. For OMV isolation, broth culture tubes were centrifuged to pellet the bacterial cells, and the supernatant was collected and filtered to remove any remaining bacterial cells. The filtrate was then subjected to ultracentrifugation to pellet the OMVs. OMVs were characterised using NTA, followed by RNA sequencing on an Illumina MiSeq platform. Small RNAs were predicted using FlaiMapper and PresRAT, and validated by qPCR.

FP G3, *FP* GIW08, IT02, IT09, IWL08, K9/00, KKOK-1706, KU060626-59, LM01-*Fp*, MH1, NNS1-1804, NNS4-1804, NO014, OSU-THCO2-90, P7-7B/10, P158B-11, P30-2B, TN, TR). The high virulent *Fp* strains included *FP* G1, *FP* S-F15, 160401-1/5N, P30-2B/09, F164, *FP* S-F16, *FP* S-S11A, 990512-1/2A, P15-8B/11, 160401-1/5M, *FP* S-F27, *FP* S-R7, *FP* S-S9, JIP02-86, *FP* S-S6, OSU THCO2-90, *FP* S-P3, *FP* S-R9, *FP* S-P1, V46, JIP 08/99, JIP 16/00) (Sundell et al., 2019), whereas less virulent *Fp* strains included *FP* S-S10, 010418-2/1, K9/00, 950106-1/1, *FP* G3 and *FP* GIW08 (Jarau et al., 2018, Sundell et al., 2019). A threshold of >95% identity and 100% query coverage were used as the cutoff values for homology.

The web server IslandViewer 4 (Integrated Interface for Computational Identification and Visualisations of Genomic Island; http://www.pathogenomics.sfu.ca/islandviewer/) (Bertelli et al., 2017) was used to identify and visualise pathogenicity islands present within the *Fp* genome sequence. Bedtools (Quinlan & Hall, 2010) was used to determine the location of sRNAs within the islands.

3 | RESULTS

3.1 | OMVs extraction and NTA

In our previous study, OMVs were isolated from bacterial cells for RNA sequencing to profile the transcriptome of the protein-coding genes in the *Fp*-OMVs versus the *Fp*-whole cell (Chapagain et al., 2023) as shown in Figure 1. *Fp* colonies grown on Tryptone Yeast Extracts (TYEs) agar plates were observed as bright yellow colonies after 5 days of incubation at 15°C. In broth culture, bacterial log phase growth was observed from day 5 until day 11 (Chapagain et al., 2023). Isolated *Fp* OMVs were observed by transmission electron microscopy (TEM) as spherical-shaped particles with an average diameter of 50–100 nm, whereas *Fp* was observed as having rod-shaped morphology with a size of approximately 3–5 μm (Chapagain et al., 2023). Consistent with our previous data, examination of the TEM images of OMVs produced from two strains of *Acinetobacter baumannii*, Gram-negative, revealed that each strain produces OMVs ranging from 30 to 140 nm in diameter (Li et al., 2015). In this study, we used the Nanoparticle Tracking Analyzer to accurately characterise the vesicles (Figure 2a,b). The average size of the isolated OMVs was 235.9 ± 0.64 nm [mean ± standard error of the mean] (Figure 2b). We also sought to further characterise the *Fp* sRNAs and investigate their abundance in the OMVs versus the Fp whole cell. The experimental design is depicted in Figure 1.

3.2 | RNA-Seq identifies sRNAs enriched in OMVs

Total RNA isolated from *Fp* whole-cells and OMVs was sequenced, yielding 60,352,578 and 55,722,742 sequence reads, respectively. High-quality reads from whole-cell and OMVs were separately mapped to the *Fp* reference genome, where 80.0% and

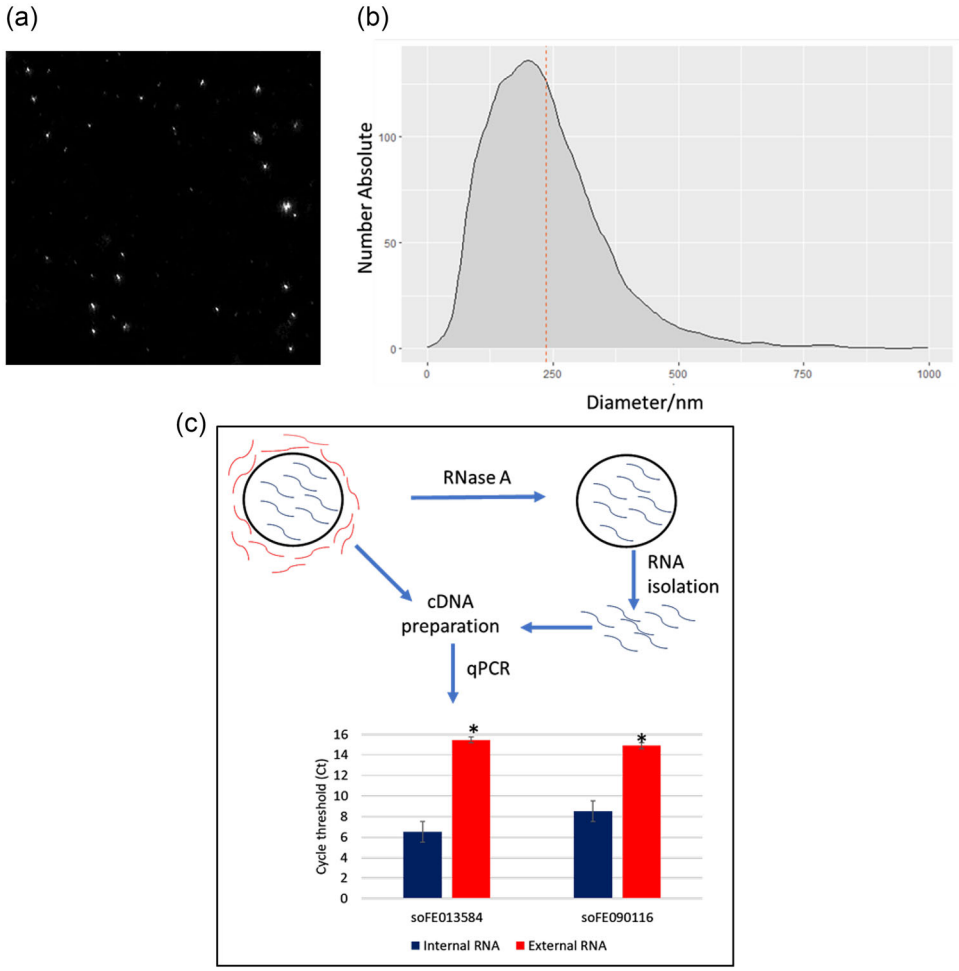

FIGURE 2 (a) A high-quality image showing properly diluted scattered OMVs tracked using Nanoparticle Tracking Analysis (NTA). (b) The absolute number of particles of each diameter is plotted. The plot displays a single peak that represents the most frequently measured size of particles, which is slightly smaller than the average size of 235.9 nm indicated by the red dots. (c) RNase A facilitates degradation of free RNA associated with the external surface of OMVs, whereas internal RNA in intact OMVs is protected from degradation. RNA attached to the OMV surface (external) and isolated from the intact, RNase A-treated OMVs (internal) were used to quantify the abundance of *soFE013584* and *soFE090116*. The sRNAs were significantly more abundant (indicated by lower CT values) inside OMVs (p-value ≤ 0.01).

80.3% read mapping rates were achieved, respectively. FlaiMapper (Hoogstrate et al., 2015) was used to predict small RNAs from the alignment files. Transcripts longer than 500 bp were filtered out, yielding 118,305 and 133,815 predicted sRNAs from the whole-cells and OMVs, respectively. The sRNA length ranged from 87 to 499 nucleotides (Average 100.4 nt). The majority of the predicted sRNAs (98.9%) were ≤100 bp in length. Large numbers of sRNAs were previously reported in OMV, (481K) in *Pseudomonas aeruginosa* (Koeppen et al., 2016). However, to further validate the predicted sRNAs, PresRAT (Kumar et al., 2021) was used to calculate a combined score (sRNA score) for each sRNA sequence using sequence score, U-richness score and average base energy and average loop energy of local minima secondary structure conformations (see methods section). Based on the calculated sRNA score, 6440 and 5537 high-confidence sRNAs were identified from the OMV and whole-cell, respectively. The predicted sRNAs with their genomic location and attributes are included in Additional file 1 (Tables S1 and S2). Various methods were used to predict sRNA candidates from datasets of *Salmonella enterica* and *Escherichia coli* (Leonard et al., 2019). The total number of sRNAs varied significantly depending on the algorithm used, ranging from around a hundred (Rockhopper) to nearly 20,000 (sRNA-Detect), with APERO yielding intermediate results (Leonard et al., 2019).

RNA-Seq of the whole-cell and OMVs revealed 499 and 592 high-confidence sRNAs, respectively, with Transcripts Per Million (TPM) expression level greater than 0.5. Of them, 279 sRNAs in OMVs and 261 sRNAs in the whole cell had TPM >1. The expression value of sRNAs in OMVs and the whole-cell are included in Additional file 1 (Tables S1 and S2). sRNAs were classified as OMV-specific when OMV sRNAs share less than 90% sequence overlap with sRNAs in the whole cell. Otherwise, they were considered 'common' sRNAs. We reported the sRNAs classification in Additional file 1 (Tables S3 and S4). In total, 958 high-confidence OMV-specific sRNAs were identified (Table 1 and Additional file 1; Table S3). Also, common sRNAs were classified

TABLE 1 Expression and genomic location of a subset of high-confidence OMV-specific sRNAs; PAI denotes sRNAs located in Pathogenicity Islands.

sRNA	Start	End	length	TPM	PAI	sRNA score
soFE129980	607022	607121	100	829.95	Yes	3.13
soFE005824	1180568	1180667	100	1.86	No	3.57
soFE124131	2532058	2532157	100	1.06	No	3.20
soFE009066	2542664	2542763	100	0.84	No	4.67
soFE125260	595778	595888	111	0.81	Yes	4.42
soFE069865	2471256	2471355	100	0.76	No	3.29
soFE002719	592543	592643	101	0.54	Yes	4.24
soFE121564	1661037	1661136	100	0.30	Yes	4.23
soFE037856	678722	678821	100	0.13	Yes	3.76
soFE034166	596554	596769	216	0.10	Yes	3.52

Note: All sRNAs were predicted by two methods.

TABLE 2 A subset sRNAs exhibiting enriched expression in the OMVs compared to the whole-cell.

sRNA	Start	End	TPM (OMV)	TPM (cell)	$\log_2$ ratio	sRNA score	PAI
soFE000208	2080699	2080798	822.14	7.66	6.75	3.31	No
soFE044277	1814045	1814144	2.69	0.02	7.16	3.26	No
soFE039138	597080	597179	1.12	0.07	4.01	6.39	Yes
soFE086681	596975	597085	1.05	0.05	4.26	6.79	Yes
soFE003644	2364152	2364251	1.05	0.05	4.42	3.21	No
soFE037172	2058129	2058228	0.79	0.01	5.89	3.16	No
soFE059881	2058153	2058252	0.78	0.01	5.86	3.62	No
soFE004683	1211780	1211879	0.76	0.02	5.31	3.29	No
soFE022545	2058177	2058276	0.75	0.06	3.77	3.57	No
soFE041581	2058192	2058300	0.73	0.06	3.71	3.89	No
soFE016429	2058122	2058221	0.73	0.01	5.76	3.50	No
soFE013584	2196236	2196335	0.17	0.02	3.09	6.91	No
soFE090116	2061593	2061691	0.12	0.03	2.09	5.24	No

Note: Log_2 ratio is the logarithmic value obtained by dividing the TPM expression of each sRNA in OMVs by that of the whole cell. PAI denotes sRNAs located in Pathogenicity Islands.

as OMV-enriched if their TPM expression was at least two times higher than the whole cell ($\log_2$ TPM ratio $\geq$1). 17.09% of the sRNAs were OMV-enriched (Table 2 and Additional file 1; Table S4).

To validate OMV-packaged sRNAs, two sRNAs (*soFE013584* and *soFE090116*) were quantified inside and outside the OMVs by qPCR (Figure 2b). We used the membrane-impermeable RNase A, which can degrade RNAs adherent to the external surface of OMVs without penetrating the vesicles. OMV-associated RNAs were visualised on agarose gel (data not shown). sRNA quantification was performed in triplicates by using RNA isolated from RNase-untreated versus-treated OMVs. RNase digestion of the external RNA revealed a high abundance of sRNAs *soFE013584* and *soFE090116* inside OMV that is, in RNase-treated OMVs compared to RNase-untreated OMVs (Figure 2b). Before performing qPCR, we tested whether exposure of OMVs to 42°C during cDNA preparation affects the OMVs stability and quantity of RNA adherent to the OMV external surface. There was no significant difference between the RNA quantities before and after exposure to 42°C (11.7 vs. 9.4 ng/μL; p-value = 0.47), indicating stability of the OMVs at 42°C. This result agrees with the notion that OMVs remain intact under different treatments and temperatures (reviewed in (Cai et al., 2018)). The OMV-specific or -enriched sRNAs could be explained by the selective inclusion of sRNAs in the OMV, which suggests potential roles of these sRNAs in microbe-host interaction. Consistent with our data, a previous study reported enrichment of sRNAs in *P. aeruginosa* OMVs (Koeppen et al., 2016).

3.3 | sRNAs within pathogenicity islands (PAIs)

Genomic islands were predicted in *Fp* by at least one computational method (Figure 3). The complete output table from the IslandViewer showing genomic island size, location and annotation is included in Additional file 2 (Table S5). 309

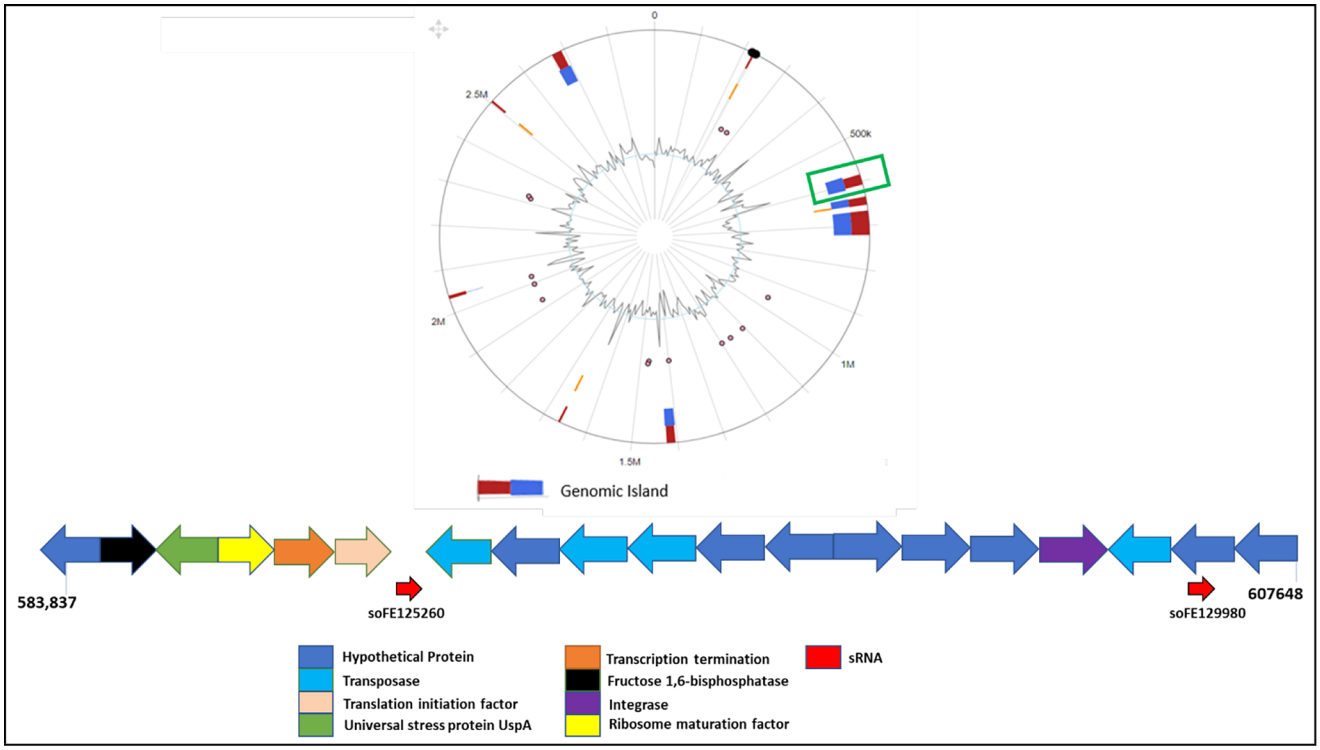

FIGURE 3 Genomic pathogenicity islands (clusters of genes that play a role in microbial adaptability) of *Fp* predicted by either IslandPath-DIMOB alone (Blue) or integrated methods (at least two methods, Red). The green window indicates the location of two sRNAs, *soFE129980* and *soFE125260*, within genomic PAIs. Color-coded arrows representing the physical location of genes within PAIs are annotated at the bottom of the figure, where the red arrows indicate sRNAs.

OMV-packaged sRNAs (Avg TPM = 67.6) were predicted in the PAIs (Additional file 2; Table S6). For instance, the OMV-specific sRNA *soFE129980* overlapped with a hypothetical protein within a PAI spanning the genomic region 583,837–607,648. Other genes within this PAI included transposase, integrase, universal stress protein UspA and transcription termination/anti-termination protein NusA (Figure 3). Also, we identified OMV-specific sRNAs, such as *soFE125260*, spanning intergenic regions within the PAIs.

sRNAs can function like eukaryotic microRNAs by binding to mRNA targets to repress translation (Koeppen et al., 2016). Due to their pathogenic potential, we thought to gain insight into the possible interaction of OMV-specific sRNAs (Table 1) with immune-related target genes in the rainbow trout host. Marancik et al. (2014) identified 2633 putative immune relevant genes by GO and manual annotations of the first draft of the trout genome (Berthelot et al., 2014). We remapped these sequences to a newer reference of the rainbow trout genome. Sequences were mapped to 2101 genomic loci. We selected the longest transcript generated from each locus to investigate the OMV sRNA-host immune gene interactions. sRNAs in Table 1 were predicted to target multiple host immune transcripts (Additional file 2; Table S7). sRNA *soFE129980* exhibited the highest-confidence interactions with immune-related genes encoding NLR family CARD domain-containing protein 3, interleukin 1 receptor-like 1 and tripartite motif-containing protein 16 (ndG <−1). Consistent with our findings, a single bacterial small RNA enriched in the OMVs has previously been shown to modify the abundance of thousands of proteins through direct and/or indirect repression of the host target proteins (Koeppen et al., 2016). These results suggest a potential role for the OMV-sRNAs in the host-pathogen interaction.

3.4 | Dual RNA-Seq of host and pathogen on day 5 post-infection of fish from resistant and susceptible genetic lines

In this study, we aimed to investigate host-pathogen interactions, in vivo, on day 5 following infection of rainbow trout with *F. psychrophilum*. In particular, we sought to investigate the correlation in expression between bacterial sRNAs and host immune-related genes that are likely targeted by these sRNAs in genetic lines with various disease susceptibility. For this purpose, we used fish collected from selectively bred resistant (ARS-*Fp* -R) and susceptible (ARS-*Fp* -S) genetic lines challenged with *Fp*

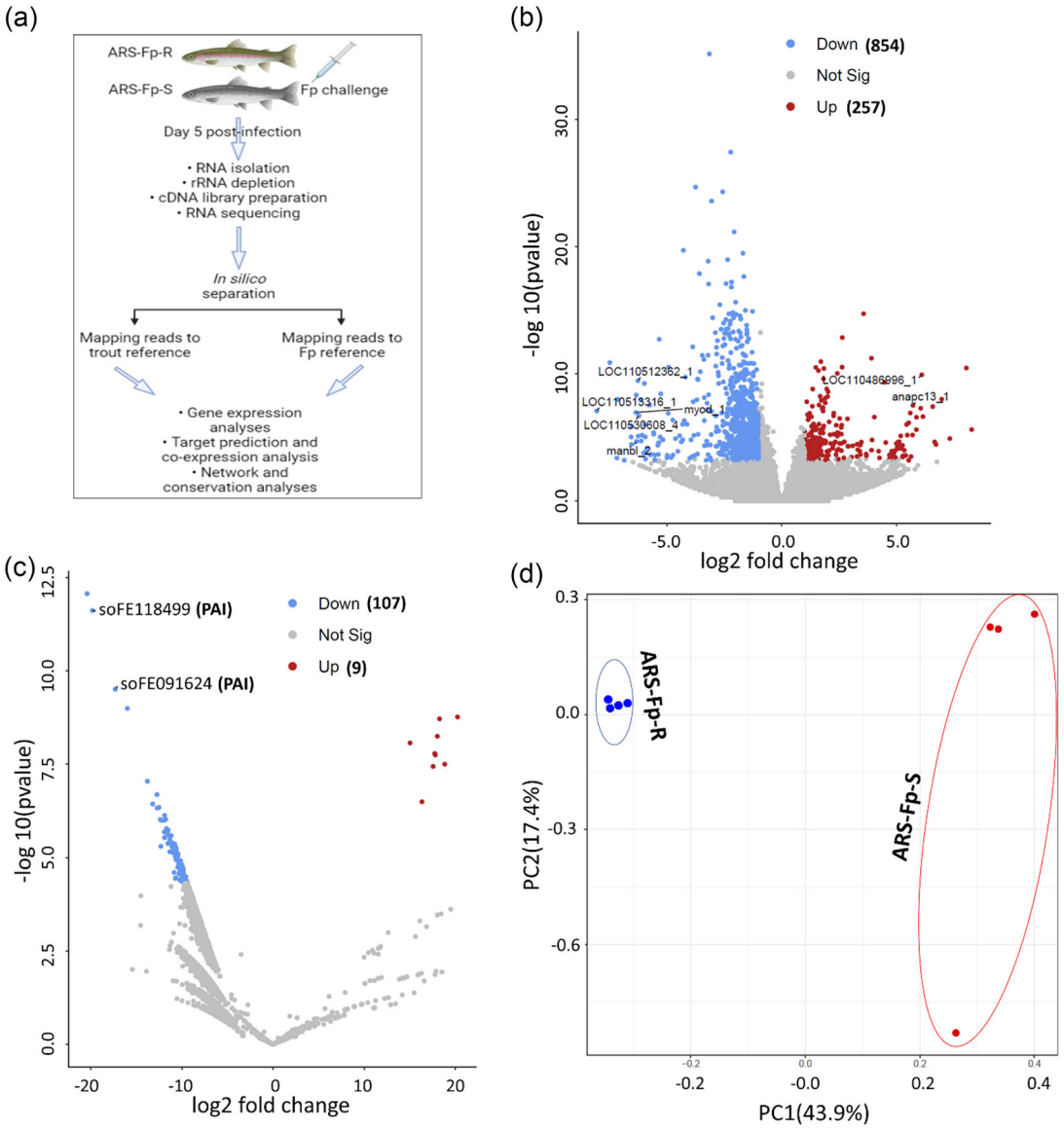

FIGURE 4 (a) Whole-body dual RNA-seq. Fish were intraperitoneally injected with *Fp* as previously described by Marancik et al. (2014). Total RNA was isolated from fish collected on day 5 post-infection and processed for sequencing. Sequence reads were separated, in silico, by mapping to the rainbow trout and *Fp* genomes to identify DE transcripts and hub genes during host-pathogen interactions. (b and c) Volcano plots showing the host transcripts (mRNAs & lncRNAs) and bacterial sRNAs, respectively, differentially expressed on day 5 following *Fp* infection in selectively bred, resistant- versus susceptible-line rainbow trout. The red dots represent the upregulated transcripts in the resistant line, whereas the blue dots represent the downregulated transcripts at FDR ≤ 0.05. Two sRNAs named in the figure, located in the PAIs, were among the most upregulated sRNAs in the susceptible genetic line. (d) Principal component analysis of OMV-specific sRNAs obtained from 8 RNA-seq datasets generated from selectively bred, resistant- and susceptible-line rainbow trout on day 5 post-infection. Each round dot represents a single RNA-seq dataset color-coded by a genetic line.

as previously described in (Marancik et al., 2014). Total RNA was sequenced for host mRNAs, lncRNAs and bacterial sRNAs (see Methods section). RNA-Seq from infected resistant and susceptible genetic lines yielded 372,100,715 raw sequence reads (average of 46,512,589 reads/sample) with ~12.1 depth of coverage. To identify differentially expressed (DE) transcripts, high-quality reads were separately mapped to the reference genomes of the host and pathogen (Figure 4a). A total of 285,744,993 (76.8%) trimmed reads were mapped to the rainbow trout genome. In our previous studies, 59.9% of the total RNA-sequence reads (518,881,838) were mapped to the trout references (Marancik et al., 2014, Paneru et al., 2016). Additionally, 4,729,437 reads (1.27%) were mapped to the *Fp* reference genome. Notably, 99.4% of the *Fp* mapped reads were generated from the susceptible genetic line, which is explained by a higher bacterial load as reported in the susceptible line compared to the resistant line (Marancik et al., 2014). Normalised gene expression was used to account for differences across samples by converting raw count data to TPM values. Quality and mapping statistics of sequence reads are given in Additional file 3; Table S8. A total of 516

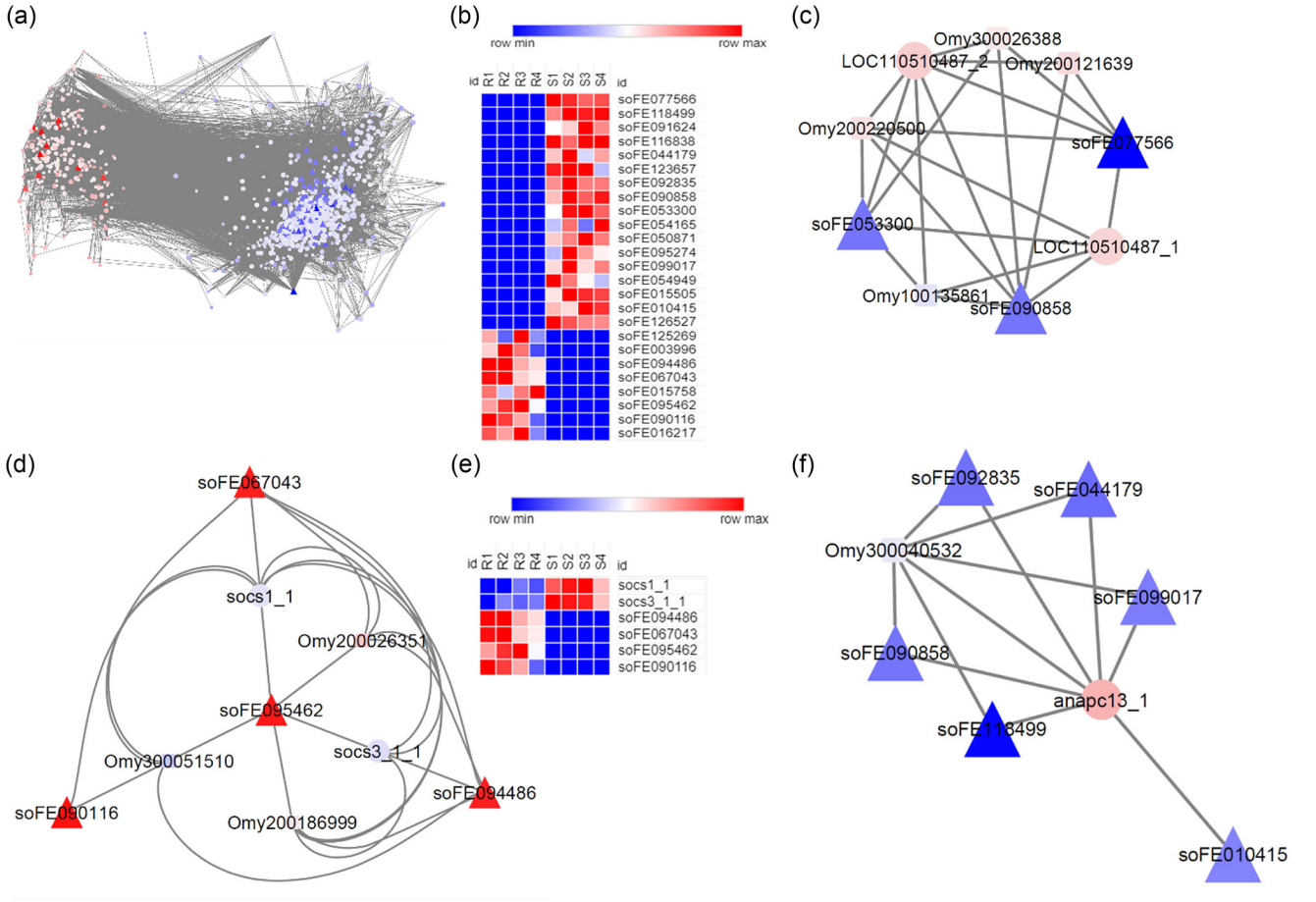

FIGURE 5 (a) Gene expression network of DE bacterial sRNAs (triangular nodes) and DE host transcripts (mRNAs 'circular nodes' and lncRNAs 'rectangular nodes') ($R > 0.85$ or <-0.85). DE transcripts are clustered into two groups based on their fold change, with the upregulated transcripts in the BCWD-resistant genetic line represented in red and the downregulated transcripts represented in blue. (b) A heat map showing the expression profile of 25 DE sRNAs between resistant (R) and susceptible (S) genetic lines. (c) Interaction network between 3 bacterial sRNAs (blue), including the OMV-specific sRNA *soFE090858*, exhibited reciprocal expression with two isoforms encoding trichohyalin (LOC110510487_1 & LOC110510487_2). (d) Interaction network between 4 sRNAs negatively correlated in expression with transcripts encoding SOCS1 & SOCS3. The SOCS transcripts were downregulated in resistant fish. The sRNA in the centre of the figure (*soFE095462*) is located in PAI. (e) A heat map showing the expression profile of the SOCS transcripts and negatively correlated sRNAs in resistant (R) and susceptible (S) genetic lines. (f) Interaction network of ANAPC13_1 (red circle); the top downregulated transcript with known functions in susceptible fish on day 5 post-infection. ANAPC13_1 exhibited target interaction and negative correlation in expression with 6 sRNAs located in PAI or enriched in OMVs. LncRNA Omy300040532 likely mediates the interaction between most of these sRNAs and ANAPC13_1.

(483 loci) protein-coding, 595 lncRNA and 116 bacterial sRNA transcripts were DE with false discovery rate (FDR) < 0.05 and a minimum $\log_2$ fold change value ≥ 1 or ≤ -1 (Figure 4b,c and Additional file 3; Tables S9, S10 and S11). Of the DE protein-coding transcripts, 82 had immune-related functions, as we previously reported (Marancik et al., 2014). Most of the DE protein-coding (86.2%) and lncRNA transcripts (68.7%) were downregulated in the resistant line. In our previous study, 54 out of 83 lncRNAs (65.1%) were downregulated on day 5 post-infection (Paneru et al., 2016). Notably, 26.5% of the differentially regulated lncRNAs previously described in (Paneru et al., 2016) were also identified in the current study, suggesting the potential role of these genes in resistance to BCWD. More information about DE transcripts is given in Additional file 3 (Tables S9, S10 and S11).

In order to gain insights into the roles of bacterial sRNAs in fish following infection, we profiled their expression in resistant and susceptible genetic lines (Figure 4c) and then investigated their expression correlation with the host genes (Figure 5a and Additional file 3; Tables S12 and S13). Interestingly, a significant difference in the OMV-specific sRNA expression was detected between the genetic lines on day 5 following infection, with principal component analysis showing primary axis accounting for ~44% of the variation (Figure 4d). The pairwise comparison revealed 116 sRNAs with differential abundance between fish from the two genetic lines following infection (Additional file 3; Table S11); of them, 28 DE sRNAs were OMV-specific. Figure 5b shows the expression profile of 25 DE sRNAs predicted using the two prediction methods. Out of 25 DE sRNAs, 17 sRNAs (68.0%) were upregulated in susceptible fish. The DE sRNAs exhibited reciprocal expression correlation ($R < -0.85$) and predicted target interaction (ndG ≤ -0.1) with 286 DE host protein-coding transcripts (Additional file 3; Table S12). For instance, the OMV-specific

sRNA *soFE090858* exhibited reciprocal interaction with two isoforms encoding trichohyalin (Figure 5c). Trichohyalin has an essential role in the proliferation and anti-apoptosis of human keratinocytes (Makino et al., 2020), which previously demonstrated a capacity to kill bacteria (Kisich et al., 2007). BCWD causes caudal lesions in rainbow trout, and thus the upregulation of trichohyalin in resistant fish may represent a defence mechanism against the pathogen. On the other hand, 22 DE bacterial sRNAs (88.0%) were correlated in expression and predicted to interact with 42.2% of the host DE lncRNAs (ndG ≤ -0.2) (Additional file 3; Table S13). Four of the hosts' lncRNAs showed expression correlation and interaction with the host trichohyalin isoforms and bacterial sRNAs (Figure 5c and Additional file 3; Tables S13 and S14).

Among the differentially regulated protein-coding transcripts, 445 (86.2%) were downregulated in the resistant line (Additional file 3; Table S9). Of note, seven transcripts encoding suppressor of cytokine signalling 1 and 3 (SOCS1&3) were upregulated in the susceptible genetic line. *Mycobacterium tuberculosis* induced early expression of a member of the SOCS family to control phagosomal acidification by selectively targeting the ATP6V1A for degradation (Queval et al., 2017). SOCS1-deficient mice exhibited increased phagocytosis and decreased bacterial loads (Klopfenstein et al., 2020). This mechanism may help explain the high bacterial load in the susceptible genetic line compared to the resistant line. Four upregulated sRNAs in resistant fish showed interaction and correlation in expression with transcripts encoding SOCS1 and SOCS3 (Figure 5d,e). For instance, the OMV-packaged sRNA *soFE090116* was negatively correlated in expression with the SOCS1 (Figure 5d). Also, the list of DE transcripts included histone H3, MYOD, C-X-C motif chemokine 11, cathelicidin antimicrobial peptide and hepcidin. Histone H3 ($\log_2$FC $= -8.05$) and MYOD ($\log_2$FC $= -6.3$) were at the top of the downregulated genes in the resistant line. Pathogens, such as bacteria, reprogram the host cells during infection through the induction of histone H3 modifications, which modulate the host transcription machinery (Dong et al., 2020).

In contrast, only 71 upregulated host transcripts were identified in resistant fish (Additional file 3; Table S9). Uncharacterised LOC110486996 and anaphase-promoting complex subunit 13 (ANAPC13_1) were the most highly upregulated transcripts. ANAPC13 is involved in cell cycle progression and has been reported to have a potential role in class-I MHC-mediated antigen presentation (Abbas et al., 2020). ANAPC13_1 exhibited interaction and reciprocal expression with 6 sRNAs (Figure 5f). Of them, the OMV-enriched sRNA *soFE118499* was located in PAI (Additional file 2; Table S6), whereas the 5 other sRNAs were either OMV-specific or -enriched (Additional file 1; Table S3). Of note, most of the sRNAs were more likely interacting with ANAPC13_1 through lncRNA Omy300040532, which negatively correlates in expression with ANAPC13_1 (Figure 5f).

3.5 | Conservation of DE sRNAs in 65 strains with variable degrees of virulence

We investigated the conservation of 25 DE high-confidence sRNAs in 65 strains with variable degrees of virulence. Based on previous studies, 23 *Fp* strains were categorised as high virulent strains, and six strains were categorised as low virulent strains (see Methods section) (Castillo et al., 2016, Jarau et al., 2019, Sundell et al., 2019). Of 25 DE sRNAs, a single DE sRNA (*soFE095274*) is conserved in all tested strains, whereas three DE sRNAs are present in the virulent strains. The list of sRNAs belonging to each group is included in Additional file 3 (Table S15).

Among sRNAs present in virulent strains, a single sRNA (*soFE015758*) was located within a PAI spanning the genomic region 583837–607648. sRNA *soFE015758* has many predicted immune gene targets, including dedicator of cytokinesis protein 2, leucine-rich repeats and immunoglobulin-like domains protein 1, and tumour necrosis factor-alpha-induced protein 2.

3.6 | In vitro treatment of RTgill-W1 cells with OMVs

A cell viability assay was performed to determine whether OMVs induce cytotoxicity in RTgill-W1 cells after different time durations of treatment (Figure 6a). A Presto Blue cell viability assay showed significant cytotoxicity after OMV exposure of 12 and 24 h (Figure 6b). The cytotoxic effect of OMVs on host cells might be mediated by the enzymes or toxins incorporated in OMVs.

To further gain insights into the molecular mechanism of interaction between OMVs and host cells, we profiled transcriptome expression of RTgill-W1 cells at 24 h post-treatment with OMVs (Figure 6c). RNA sequencing yielded 105,955,286 reads (Average of 17,659,214 reads) from six cDNA libraries prepared from control and treated cells (3 libraries/each). A total of 77,160,290 (72.82%) reads were mapped to the rainbow trout genome. 152 trout transcripts were DE in response to OMV treatment (Figure 6d and Additional file 3; Table S16). Most of them (~66%) were upregulated in treated cells.

Remarkably, our analysis of the RTgill-W1 cell response to OMV treatment after 24 h, considered an early response (Ali & Salem, 2022, Marancik et al., 2014), did not reveal signs of downregulation of host genes with potential roles in immunity. Only a single gene, complement factor H was downregulated in treated cells (Additional file 3; Table S16). Pathogens exploit complement factor H to inhibit opsonisation by C3, and thus resist phagocytosis (Pandiripally et al., 2003). Conversely, we observed upregulated expression of several immune-related genes such as complement protein component C7-1, chemokine CXCF1b,

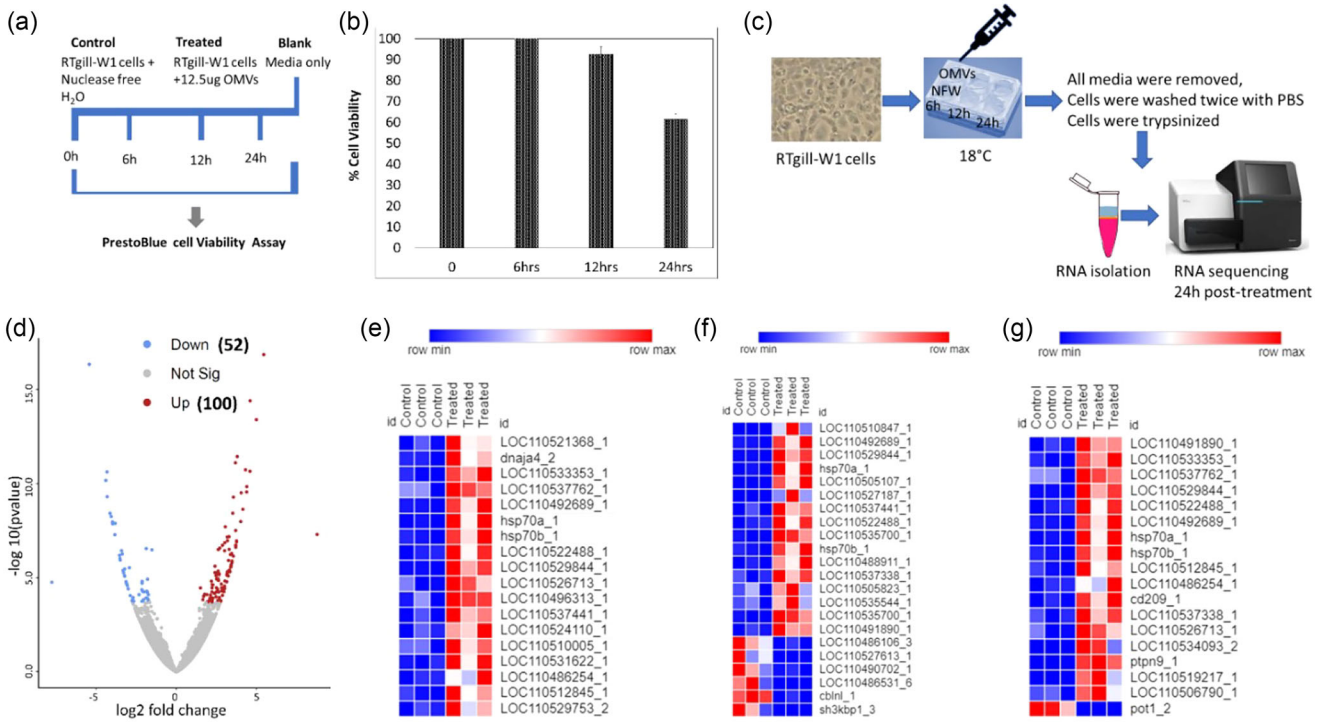

FIGURE 6 (a) Overview of PrestoBlue cell viability assay in RTgill-W1 cells after different time durations of OMVs treatment. Approximately 500,000 cells/well were seeded in 96-well plates for 24 h. Cells were then treated with OMVs or Nuclease-free water (NFW; control group) for 0 min, 6, 12 and 24 h at 18°C. Cell culture medium was used as a blank for the PrestoBlue Assay. PrestoBlue reagent was added to wells, followed by incubation at appropriate temperatures and absorbance measurement at 570 nm wavelength to determine cell viability. (b) PrestoBlue cell viability assay in OMVs treated RTgill-W1 cells showed that the cytotoxicity increases with increased time duration of OMVs exposure. Significant cytotoxicity was observed at 12 and 24 h ($p < 0.05$). (c) Approximately 1.2×10^6 RTgill-W1 cells/well were seeded in 6-well tissue culture plates and maintained overnight at 18°C. Cells were exposed to either OMVs or NFW (control group) for 6, 12 and 24 h at 18°C. The media from the 'control' and 'treated' cell wells were removed, and cells were washed, trypsinised and then lysed with Trizol reagent for RNA extraction and sequencing on day 1 post-treatment. (d) A Volcano plot showing the host transcripts DE on day 1 following OMVs treatment in RTgill-W1 cells. The red dots represent the upregulated transcripts in the OMV-treated cells, whereas the blue dots represent the downregulated transcripts at FDR ≤0.05. Heat maps showing DE transcripts involved in chaperones and folding catalysts (e), membrane trafficking and endocytic pathway (f) and phagocytosis and antigen processing and presentation (g).

TNFAIP3-interacting protein 1, and transcription factor AP-1 (Additional file 3; Table S16). C7 molecule is a constituent of the membrane attack complex (MAC), which forms pores into bacterial target membranes, leading to cell lysis and death (Sundell et al., 2019).

The KEGG analysis provided a general overview of essential genes/pathways showing DE following OMV treatment. Genes involved in chaperones and folding catalysts, membrane trafficking and endocytic pathway, phagocytosis, and antigen processing and presentation were upregulated (Figure 6e–g and Additional file 3; Table S16). Also, 12 transcripts encoding Hsp70, Hsp90 and cochaperones were upregulated in RTgill-W1cells in response to OMV treatment (Figure 6e).

In addition, some proteins involved in endosomal trafficking were upregulated, including Rab and vacuolar protein sorting proteins. Upregulation of lysosomal-associated membrane protein 2 (LAMP2), ras-related protein Rab-5A (Rab5a) and ras-related protein Rab-7a (Rab7a) was detected by qPCR. Contrariwise, we noticed downregulation of a few endocytosis-related genes such as PH and SEC7 domain-containing protein 1, protein CLEC16A and SH3 domain-containing kinase binding protein 1 (sh3kbp1) (Figure 6f). Figure 6g shows seven upregulated genes implicated in phagocytosis. The list includes genes essential for pathogen recognition (CD209 molecule), actin remodelling (fibroblast growth factor 7 and transgelin-2) and phagosome acidification (V-type proton ATPase catalytic subunit A; ATP6V1A).

Similar to the response of resistant fish to *Fp* infection shown above, OMV treatment showed early inhibition of SOCS1 at 24 h, which may indicate induction of phagosomal maturation (Queval et al., 2017). We also noticed downregulation of a transcript encoding protection of telomeres 1 (POT1), which negatively regulates phagocytosis. Additionally, ten upregulated genes involved in antigen processing and presentation were identified. These genes encode beta-2-microglobulin (B2M) and nine heat shock proteins (Figure 6g).

Furthermore, genes with anti-apoptotic roles, such as AP-1 proteins, DNA-damage-inducible transcript 4 (DDIT4), heat shock proteins (Hsp70 and Hsp90) and cochaperones (DnaJ/Hsp40 and tetratricopeptide repeat (TPR)), were upregulated (Additional

TABLE 3 OMV-enriched/-specific versus whole cell-enriched bacterial sRNA detected 24 h following treatment of the RTgill-W1 cells with OMVs.

ID	Start	End	Read counts	Category (log2 ratio)	PAI	sRNA status (score)
soFE125269	1637553	1637893	3145	cell-enriched (−1.72)	No	Yes (7.77)
soFE004028	2056951	2057269	2062	OMV-specific	No	No
soFE013584	2196235	2196334	1912	OMV-enriched (3.1)	No	Yes (6.91)
soFE002123	2061751	2061850	1020	OMV-enriched (4.23)	No	No
soFE104747	1635059	1635287	918	OMV-specific	No	Yes (6.73)
soFE048173	2195010	2195109	657	OMV-enriched (4.21)	No	No
soFE011466	597087	597258	272	cell-enriched (-1.43)	Yes	Yes (7.13)
soFE091624	595998	596220	264	OMV-enriched (1.61)	Yes	Yes (6.54)
soFE004713	1634302	1634689	231	OMV-specific	No	Yes (3.60)
soFE100359	593374	593473	216	cell-enriched (−1.31)	Yes	No
soFE073471	2540111	2540210	210	OMV-enriched (1.63)	No	Yes (7.02)
soFE011096	2046508	2046607	181	cell-enriched (−1.2)	No	No
soFE100358	593129	593228	133	OMV-specific	Yes	No

Note: The negative log2 ratio indicates that sRNA is less abundant in OMV than in the whole cell.

file 3; Table S16). However, a few genes whose products likely have apoptotic properties, such as MAP/microtubule affinity-regulating kinase 4 and Growth arrest and DNA-damage-inducible protein GADD45 beta, exhibited contrasting expression (Additional file 3; Table S16).

The OMV treatment led to the upregulation of genes implicated in the phagocytosis process. In addition, OMV-treated cells similar to the *Flavobacterium*-challenged resistant fish exhibited downregulation of the host gene encoding SOCS1. The OMV-treated cells downregulation of SOCS1 was a −220.14 fold change. SOCS1-deficient mice exhibited increased phagocytosis, bacterial killing and decreased bacterial loads (Klopfenstein et al., 2020). On the other hand, although susceptible fish had a high bacterial load, they did not demonstrate upregulation of the phagocytic pathway to degrade the pathogen, and their SOCS gene expression was higher than the resistance fish. Taken together, these results thus allowed us to propose a model for the control of phagosomal maturation by *Flavobacterium* infection and OMVs treatment (Figure 7).

Notably, 69 bacterial sRNAs showed significant abundance (>100 reads) in the treated cells. Of them, 7 sRNAs belong to the cell-enriched or OMV-enriched/-specific categories (Table 3). The top four sRNAs showed predicted target interaction with most of the downregulated host transcripts following OMV treatment. Further experimental work is needed to provide insights into the potential interaction of these sRNAs with the host genes involved in the endocytic pathway following OMVs treatment.

4 | DISCUSSION

Several studies have focused on the role of eukaryotic membrane vesicles carrying nucleic acid content (DNA, RNA, miRNA) in disease states (van den Boorn et al., 2013). However, little is known about the role of nucleic acids in prokaryotic membrane vesicles, especially in host-pathogen interactions. Previous studies have demonstrated the presence of DNA, peptidoglycan and lipopolysaccharides (LPS) in OMVs purified from bacterial cultures (Renelli et al., 2004, Turnbull et al., 2016). These cargos can be delivered to host cells by binding OMVs to surface receptors on host cells or through endocytosis (Anand & Chaudhuri, 2016, Kaparakis-Liaskos & Ferrero, 2015). Because OMVs enable the transfer of various inner constituents from bacteria to the host, it has driven our attention further to investigate the effect of OMVs on host-pathogen interactions (Chapagain et al., 2023). Thus far, only a few studies (Choi et al., 2017, Koeppen et al., 2016) have associated the presence of sRNAs within bacterial OMVs with a role in host health. Dual RNA-seq identified sRNAs produced from *Salmonella enterica*, such as *PinT*, demonstrated a role in regulating the expression of host genes and mediating the activity of virulence genes necessary for intracellular survival of the pathogen (Westermann et al., 2016). Koeppen *et al.* reported that *P. aeruginosa* sRNAs target kinases in the LPS-stimulated MAPK signalling pathway (Koeppen et al., 2016). sRNAs in the plant pathogen *Xanthomonas compestris pv vesicatoria* were also involved in pathogenicity, and deletion of the sRNA led to a reduction in virulence of bacteria (Abendroth et al., 2014).

In this study, RNA-Seq analysis revealed the presence of sRNAs in OMVs and found variation in sRNA abundance between OMV and whole-cell transcriptome. Our results indicated the existence of OMV-specific/enriched sRNAs and bioinformatically predicted their target immune-relevant genes. These sRNAs included *soFE013584* and *soFE090116*, which targets SOCS1.

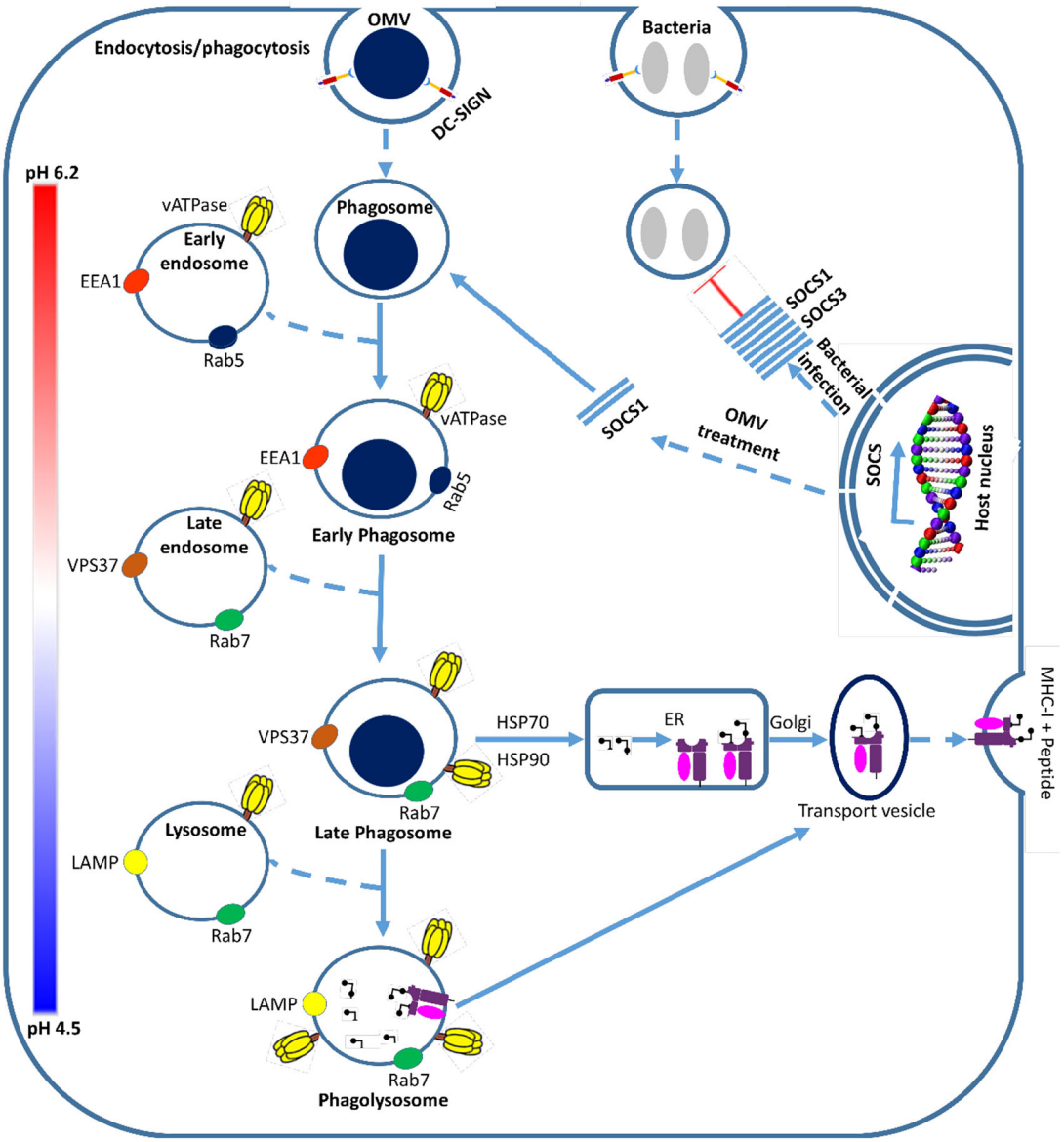

FIGURE 7 A proposed model showing modulation of the endocytic pathway by bacteria and OMVs under reciprocal regulation of SOCS1. Bacteria likely suppress phagosome maturation and lysosome fusion by upregulating the expression of the host SOCS1, as reported in Klopfenstein et al. (2020). On the contrary, phagosome maturation is likely enhanced by the downregulation of the host SOCS1 in response to OMVs treatment. The phagosome acquires Rab5 and EEA1 via fusion with early endosomes. Upregulation of EEA1 triggers fusion of the phagosome and late endosome. During the phagosome maturation process, a suite of other proteins is recruited, including Rab7, V-ATPase and lysosome-associated membrane glycoprotein (LAMP), which facilitates the fusion of lysosomes with the mature phagosome forming a phagolysosome. Degraded antigenic peptides by the proteasome (cytosolic pathway; not shown) are transported to the endoplasmic reticulum (ER) and loaded onto MHC-I molecules. Whereas degraded antigenic peptides by phagosome (vacuolar pathway) can be loaded onto itinerant MHC-I molecules within the phagosome. Dashed arrows indicate processes suggested in this study, and solid arrows refer to processes supported by information from the literature.

Similar to our work, a recent study used RNA-Seq to characterise OMVs-packaged sRNAs in *P. aeruginosa* and predicted their human immune transcript target. The study reported a specific OMV-sRNA delivered to host cells, resulting in OMV-induced attenuation of IL-8 secretion and neutrophil infiltration in mouse lungs (Koeppen et al., 2016).

Although many attempts have been made to understand the mechanism of host-pathogen interactions between rainbow trout and *Fp* (Ali et al., 2021, Marancik et al., 2014, Paneru et al., 2016), very little is known regarding the pathogenesis of this bacterium. Differential expression of trout genes between the resistant ARS-*Fp* -R and susceptible ARS-*Fp* -S genetic lines has been previously reported (Marancik et al., 2014). However, the bacterial sRNAs expression and their correlation with the rainbow trout host genes were not previously reported in rainbow trout. Our study showed that most DE sRNAs were upregulated in fish susceptible to BCWD. OMV-enriched sRNAs exhibited strong interactions and differential reciprocal expression with trout genes in BCWD-resistant and -susceptible genetic lines. sRNAs interacting with the trout genes share complementary sequences, which

might cause post-transcriptional repression of the trout genes as sRNAs can act as eukaryotic microRNAs (Wang et al., 2015). Previous studies showed that sRNAs targeting immune genes might help the bacteria to hijack the immune response and modulate the survival of bacteria in the host (Soares-Silva et al., 2016). The effect of sRNAs was also tested in *S. aureus* by silencing the sRNA, which modulated the virulence and disease resistance of *S. aureus* (Sjostrom et al., 2015). Similarly, another study in *S. aureus* reported the role of sRNA in bacterial virulence and in regulating the expression level of an immune evasion molecule (Chabelskaya et al., 2010). The current study bioinformatically predicted immune genes targeted by bacterial sRNA. Further validation studies beyond the scope of this study are warranted.

The study revealed OMV-induced cytotoxicity at 12 and 24 h following in vitro exposure of RTgill-W1 cells to 12.5 μg/mL OMVs. Consistently, *Burkholderia cepacia* OMVs induced cytotoxicity in host cells treated with ≥10 μg/mL of OMVs for 24 h (Kim et al., 2020). In addition, OMVs induced cytotoxicity of the salmonid CHSE-214 cells (Oliver et al., 2016). Most of the DE transcripts involved in cell death regulation are encoding products with anti-apoptotic roles, suggesting that cell death occurred by necrosis due to exposure to OMV toxins. One characteristic of the OMV treatment is the upregulation of transcripts for HSP70, HSP90 and cochaperones. Cochaperones, such as DnaJ/Hsp40 and tetratricopeptide repeat (TPR), determine the multifunctional properties of Hsp70 and Hsp90, including their anti-apoptotic functions (Takayama et al., 2003). The virulence factor Hsp60 was identified in the proteome of OMVs of the fish pathogen *Piscirickettsia salmonis[11]*. In addition to regulating cell death/apoptosis, heat shock proteins stimulate elements of innate immunity and traffic antigens into antigen-presenting cells, which facilitates the induction of specific acquired immune responses (reviewed in (Colaco et al., 2013)).

Moreover, OMV treatment modulated host gene expression, favouring elements from the phagocytic, endocytic and antigen presentation pathways. Phagocytosis is a conserved defence strategy in which host cells engulf and destroy self/nonself antigens. Although the epithelial RTgill-W1 cells are not professional phagocytes, epithelial cells were previously reported to have low phagocytic activity and a significant contribution to pathogen clearance (Sharma et al., 2020). Following OMV treatment, RTgill-W1 cells upregulated the phagocytic receptor CD209 (DC-SIGN), responsible for pathogen recognition (Uribe-Querol & Rosales, 2020). Upregulation of genes involved in regulating actin cytoskeleton, such as fibroblast growth factor and Transgelin-2, suggests that actin remodelling is essential at the site of phagocytosis. It has been previously reported that Transgelin-2 (Jo et al., 2018) and fibroblast growth factors (Ichinose et al., 1998, Mendoza et al., 1990) enhance phagocytosis. Several other genes involved in phagocytosis, including ATP6V1A, were also upregulated. V-ATPase molecules accumulate on the phagosomal membrane to acidify the phagosome interior (Kinchen & Ravichandran, 2008, Marshansky & Futai, 2008). Some pathogenic bacteria (*M. tuberculosis*) have developed a strategy to survive inside host phagocytes by inducing early expression of a member of the SOCS family of proteins, which controls phagosomal acidification by selectively targeting the ATP6V1A for ubiquitination (Queval et al., 2017). Consistent with the upregulation of genes implicated in the phagocytic pathway, particularly ATP6V1A, SOCS1 was dramatically downregulated in host cells in response to OMV treatment. Similarly, SOCS1 and SOCS3 were downregulated in Flavobacterium-infected resistant fish, which may explain the low bacterial load. In addition to phagocytosis, genes implicated in the endocytic pathway, such as early endosome antigen 1 (EAA1), vacuolar sorting proteins and Rab proteins, were also upregulated in response to OMV treatment. EAA1 is recruited to the phagosome, promoting early endosomal fusion with the new phagosome (Christoforidis et al., 1999).

Moreover, OMV-treated cells upregulated B2M, a scaffolding protein that retains the native structure of MHC class I molecules on the surface of nucleated cells to present antigens to cytotoxic CD8+ T cells. In addition to the role of B2M in adaptive immunity, it possesses antimicrobial activities (i.e., innate response). B2M sheds sB2M-9 fragments, which function as antibacterial chemokines, and perhaps as potential antimicrobial peptides (AMPs) following modification by thioredoxin (Chiou et al., 2021). Upregulating the expression of phagocytosis-, endocytosis- and antigen presentation-related genes may lead to increased uptake of OMVs by host cell which present processed antigens and stimulate the immune response.

OMVs possess inherent characteristics that qualify them as vaccine candidates (reviewed in (Cai et al., 2018)). For instance, OMVs are storage containers that can remain intact under different treatments and temperatures. Also, OMVs have non-living activity, adjuvant effects, non-replicative properties and hold substantial immunogenic components belonging to the parent bacteria, which may induce immune responses against bacterial infection. OMVs derived from *Salmonella* Enteritidis (Liu et al., 2017) and *Bordetella bronchiseptica* (Bottero et al., 2018) provided substantial protection against the parent bacterial infection. However, further research is still needed to study the role of *F. psychrophilum*-derived OMVs in boosting the host immune response, and thus their potential application as a vaccine to contain/control the BCWD. It is worth mentioning that the OMV treatment effects on host gene expression are considered early response compared to the late response shown in the in vivo study, the fifth day after infection in the susceptible versus resistant genetic lines.

5 | CONCLUSIONS

The current study characterised for the first time the *Fp* sRNAs in OMVs and demonstrated their correlation in expression with predicted host immune genes in vivo and in vitro. One key aspect of this study is the simultaneous capture of the RNA expression profile of the *Fp* and its fish host (rainbow trout) following infection in selectively bred resistant and -susceptible genetic lines.

The whole-body dual RNA-seq approach yielded a comprehensive transcriptomic dataset that enabled us to identify microbial factors contributing to the disease progression at a late stage of the infection. We identified bacterial sRNAs packaged/enriched within OMVs delivered to the host cells after OMV treatment. Future studies considering the early and late stages of infection will provide insights into the dynamics of gene expression changes during infection.

Additionally, the study revealed significant cell lysis/death at 12 and 24 h following in vitro exposure of RTgill-W1 cells to OMVs. Another key finding of this study is the reciprocal regulation of SOCS1 in *Flavobacterium*-infected susceptible fish and OMVs-treated host cells. The OMV treatment modulated host gene expression, favouring elements from the phagocytic, endocytic and antigen presentation pathways. Further studies are needed to investigate whether OMVs can induce immune memory in rainbow trout and thus assess their potential use as a vaccine.

AUTHOR CONTRIBUTIONS

Pratima Chapagain: Data curation (equal); formal analysis (equal); investigation (equal); methodology (equal); writing—original draft (equal). **Ali R. Ali**: Data curation (equal); formal analysis (equal); investigation (equal); methodology (equal). **Destaalem T. Kidane**: Data curation (equal); methodology (equal). **Mary Farone**: Investigation (equal); methodology (equal); resources (equal). **Mohamed Salem**: Conceptualization (lead); funding acquisition (lead); investigation (equal); project administration (lead); supervision (lead).

ACKNOWLEDGEMENTS

The authors acknowledge Dr. Gregory D. Wiens for providing *Fp* (CSF 259–93) for OMV isolation and tissues from BCWD-resistant and -susceptible genetic lines for dual RNA-Seq. Dr. Katharina Maisel and Matthew Ensign are acknowledged for their help with the Nanoparticle Tracking Analysis.

CONFLICT OF INTEREST STATEMENT

The authors declare no conflicts of interest.

DATA AVAILABILITY STATEMENT

The Raw RNA-Req data that support the findings of this study are openly available from the NCBI Short Read Archive under BioProject ID PRJNA259860 (accession number SUB10837562).

INSTITUTIONAL REVIEW BOARD STATEMENT

Fish were maintained at the NCCCWA, and animal procedures were performed under the guidelines of NCCCWA Institutional Animal Care and Use Committee Protocols #053 and #076.

ORCID

Mohamed Salem https://orcid.org/0000-0003-2142-6716

REFERENCES

Abbas, S. Z., Qadir, M. I., & Muhammad, S. A. (2020). Systems-level differential gene expression analysis reveals new genetic variants of oral cancer. *Scientific Reports*, *10*, 14667.

Abendroth, U., Schmidtke, C., & Bonas, U. (2014). Small non-coding RNAs in plant-pathogenic Xanthomonas spp. *RNA Biology*, *11*, 457–463.

Ali, A., Al-Tobasei, R., Kenney, B., Leeds, T. D., & Salem, M. (2018). Integrated analysis of lncRNA and mRNA expression in rainbow trout families showing variation in muscle growth and fillet quality traits. *Scientific Reports*, *8*, 12111.

Ali, A., & Salem, M. (2022). Genome-wide identification of antisense lncRNAs and their association with susceptibility to Flavobacterium psychrophilum in rainbow trout. *Frontiers in Immunology*, *13*, 1050722.

Ali, A., Thorgaard, G. H., & Salem, M. (2021). PacBio iso-seq improves the rainbow trout genome annotation and identifies alternative splicing associated with economically important phenotypes. *Frontiers in Genetics*, *12*, 683408.

Anand, D., & Chaudhuri, A. (2016). Bacterial outer membrane vesicles: New insights and applications. *Molecular Membrane Biology*, *33*, 125–137.

Barbier, P., Rochat, T., Mohammed, H. H., Wiens, G. D., Bernardet, J. F., Halpern, D., Duchaud, E., & McBride, M. J. (2020). The type IX secretion system is required for virulence of the fish pathogen Flavobacterium psychrophilum. *Applied and Environmental Microbiology*, *86*(16), e00799-20.

Barnes, M. E., & Brown, M. L. (2011). A review of Flavobacterium psychrophilum biology, clinical signs, and bacterial cold water disease prevention and treatment. *The Open Fish Science Journal*, *4*, 1–9.

Bertelli, C., Laird, M. R., Williams, K. P., Simon Fraser University Research Computing, G., Lau, B. Y., Hoad, G., Winsor, G. L., & Brinkman, F. S. L. (2017). IslandViewer 4: Expanded prediction of genomic islands for larger-scale datasets. *Nucleic Acids Research*, *45*, W30–W35.

Berthelot, C., Brunet, F., Chalopin, D., Juanchich, A., Bernard, M., Noel, B., Bento, P., Da Silva, C., Labadie, K., Alberti, A., Aury, J. M., Louis, A., Dehais, P., Bardou, P., Montfort, J., Klopp, C., Cabau, C., Gaspin, C., Thorgaard, G. H., … Guiguen, Y. (2014). The rainbow trout genome provides novel insights into evolution after whole-genome duplication in vertebrates. *Nature Communications*, *5*, 3657.

Bottero, D., Zurita, M. E., Gaillard, M. E., Bartel, E., Vercellini, C., & Hozbor, D. (2018). Membrane vesicles derived from Bordetella bronchiseptica: Active Constituent of a new vaccine against infections caused by this pathogen. *Applied and Environmental Microbiology*, *84*(4), e01877-17.

Cai, W., Kesavan, D. K., Wan, J., Abdelaziz, M. H., Su, Z., & Xu, H. (2018). Bacterial outer membrane vesicles, a potential vaccine candidate in interactions with host cells based. *Diagn Pathology*, *13*, 95.

Castillo, D., Christiansen, R. H., Dalsgaard, I., Madsen, L., Espejo, R., & Middelboe, M. (2016). Comparative genome analysis provides insights into the pathogenicity of Flavobacterium psychrophilum. *PLoS ONE*, *11*, e0152515.

Chabelskaya, S., Gaillot, O., & Felden, B. (2010). A Staphylococcus aureus small RNA is required for bacterial virulence and regulates the expression of an immune-evasion molecule. *Plos Pathogens*, *6*, e1000927.

Chao, Y., Papenfort, K., Reinhardt, R., Sharma, C. M., & Vogel, J. (2012). An atlas of Hfq-bound transcripts reveals 3' UTRs as a genomic reservoir of regulatory small RNAs. *Embo Journal*, *31*(20), 4005–4019.

Chapagain, P., Ali, A., & Salem, M. (2023). Dual RNA-Seq of Flavobacterium psychrophilum and its outer membrane vesicles distinguishes genes associated with susceptibility to bacterial cold-water disease in rainbow trout (Oncorhynchus mykiss). *Pathogens (Basel, Switzerland)*, *12*(3), 436.

Chen, R., Wei, X., Li, Z., Weng, Y., Xia, Y., Ren, W., Wang, X., Jin, Y., Bai, F., Cheng, Z., Jin, S., & Wu, W. (2019). Identification of a small RNA that directly controls the translation of the quorum sensing signal synthase gene rhlI in Pseudomonas aeruginosa. *Environmental Microbiology*, *21*, 2933–2947.

Chen, X. P., Ali, L., Wu, L. Y., Liu, C., Gang, C. X., Huang, Q. F., Ruan, J. H., Bao, S. Y., Rao, Y. P., & Yu, D. (2018). Biofilm formation plays a role in the formation of multidrug-resistant Escherichia coli toward nutrients in microcosm experiments. *Frontiers in Microbiology*, *9*, 367.

Chiou, S.-J., Ko, H.-J., Hwang, C.-C., & Hong, Y.-R. (2021). The double-edged sword of beta2-microglobulin in antibacterial properties and amyloid fibril-mediated cytotoxicity. *International Journal of Molecular Sciences*, *22*, 6330.

Choi, J. W., Kim, S. C., Hong, S. H., & Lee, H. J. (2017). Secretable small RNAs via outer membrane vesicles in periodontal pathogens. *Journal of Dental Research*, *96*, 458–466.

Christoforidis, S., McBride, H. M., Burgoyne, R. D., & Zerial, M. (1999). The Rab5 effector EEA1 is a core component of endosome docking. *Nature*, *397*, 621–625.

Colaco, C. A., Bailey, C. R., Walker, K. B., & Keeble, J. (2013). Heat shock proteins: Stimulators of innate and acquired immunity. *BioMed Research International*, *2013*, 461230.

Deng, Z. L., Munch, P. C., Mreches, R., & McHardy, A. C. (2022). Rapid and accurate identification of ribosomal RNA sequences via deep learning. *Nucleic Acids Research*, *50*, e60.

Dong, W., Rasid, O., Chevalier, C., Connor, M., Eldridge, M., & Hamon, M. A. (2020). Streptococcus pneumoniae infection promotes histone H3 dephosphorylation by modulating host PP1 phosphatase. *Cell Reports*, *30*(12), 4016–4026.

Dutcher, H. A., & Raghavan, R. (2018). Origin, evolution, and loss of bacterial small RNAs. *Regulating with RNA in Bacteria and Archaea*, 487–497.

Ellis, T. N., & Kuehn, M. J. (2010). Virulence and immunomodulatory roles of bacterial outer membrane vesicles. *Microbiology and Molecular Biology Reviews*, *74*, 81–94.

Gomez, E., Mendez, J., Cascales, D., & Guijarro, J. A. (2014). Flavobacterium psychrophilum vaccine development: A difficult task. *Microbial Biotechnology*, *7*, 414–423.

Gottesman, S., & Storz, G. (2011). Bacterial small RNA regulators: Versatile roles and rapidly evolving variations. *Cold Spring Harbor Perspectives in Biology*, *3*(12), a003798.

Haurat, M. F., Aduse-Opoku, J., Rangarajan, M., Dorobantu, L., Gray, M. R., Curtis, M. A., & Feldman, M. F. (2011). Selective sorting of cargo proteins into bacterial membrane vesicles. *Journal of Biological Chemistry*, *286*, 1269–1276.

Hesami, S., Metcalf, D. S., Lumsden, J. S., & Macinnes, J. I. (2011). Identification of cold-temperature-regulated genes in Flavobacterium psychrophilum. *Applied and Environmental Microbiology*, *77*, 1593–1600.

Hoogstrate, Y., Jenster, G., & Martens-Uzunova, E. S. (2015). FlaiMapper: Computational annotation of small ncRNA-derived fragments using RNA-seq high-throughput data. *Bioinformatics*, *31*, 665–673.

Ichinose, M., Sawada, M., Sasaki, K., & Oomura, Y. (1998). Effect of acidic fibroblast growth factor (aFGF) on phagocytosis in mouse peritoneal macrophages. *Microbiology and Immunology*, *42*, 139–142.

Jan, A. T. (2017). Outer Membrane Vesicles (OMVs) of Gram-negative Bacteria: A Perspective Update. *Frontiers in Microbiology*, *8*, 1053.

Jarau, M., Di Natale, A., Huber, P. E., MacInnes, J. I., & Lumsden, J. S. (2018). Virulence of Flavobacterium psychrophilum isolates in rainbow trout Oncorhynchus mykiss (Walbaum). *Journal of Fish Diseases*, *41*, 1505–1514.

Jarau, M., MacInnes, J. I., & Lumsden, J. S. (2019). Erythromycin and florfenicol treatment of rainbow trout Oncorhynchus mykiss (Walbaum) experimentally infected with Flavobacterium psychrophilum. *Journal of Fish Diseases*, *42*, 325–334.

Jo, S., Kim, H. R., Mun, Y., & Jun, C. D. (2018). Transgelin-2 in immunity: Its implication in cell therapy. *Journal of Leukoc Biology*, *104*, 903–910.

Kang, X. M., Wang, F. F., Zhang, H., Zhang, Q., & Qiana, W. (2015). Genome-wide identification of genes necessary for biofilm formation by nosocomial pathogen Stenotrophomonas maltophilia reveals that orphan response regulator FsnR is a critical modulator. *Applied and Environmental Microbiology*, *81*, 1200–1209.

Kaparakis-Liaskos, M., & Ferrero, R. L. (2015). Immune modulation by bacterial outer membrane vesicles. *Nature Reviews Immunology*, *15*, 375–387.

Kim, D., Pertea, G., Trapnell, C., Pimentel, H., Kelley, R., & Salzberg, S. L. (2013). TopHat2: Accurate alignment of transcriptomes in the presence of insertions, deletions and gene fusions. *Genome Biology*, *14*, R36.

Kim, S. Y., Kim, M. H., Son, J. H., Kim, S. I., Yun, S. H., Kim, K., Kim, S., Shin, M., & Lee, J. C. (2020). Outer membrane vesicles produced by Burkholderia cepacia cultured with subinhibitory concentrations of ceftazidime enhance pro-inflammatory responses. *Virulence*, *11*, 995–1005.

Kinchen, J. M., & Ravichandran, K. S. (2008). Phagosome maturation: Going through the acid test. *Nature Reviews Molecular Cell Biology*, *9*, 781–795.

Kisich, K. O., Howell, M. D., Boguniewicz, M., Heizer, H. R., Watson, N. U., & Leung, D. Y. (2007). The constitutive capacity of human keratinocytes to kill Staphylococcus aureus is dependent on beta-defensin 3. *The Journal of Investigative Dermatology*, *127*, 2368–2380.

Klopfenstein, N., Brandt, S., & Serezani, C. H. (2020). Phagocyte-derived SOCS1 disrupts Staphylococcus aureus skin host defense. *The Journal of Immunology*, *204*, (1_Supplement), 227–4.

Koeppen, K., Hampton, T. H., Jarek, M., Scharfe, M., Gerber, S. A., Mielcarz, D. W., Demers, E. G., Dolben, E. L., Hammond, J. H., Hogan, D. A., & Stanton, B. A. (2016). A novel mechanism of host-pathogen interaction through sRNA in bacterial outer membrane vesicles. *Plos Pathogens*, *12*, e1005672.

Kumar, K., Chakraborty, A., & Chakrabarti, S. (2021). PresRAT: A server for identification of bacterial small-RNA sequences and their targets with probable binding region. *RNA Biology*, *18*, 1152–1159.

Leonard, S., Meyer, S., Lacour, S., Nasser, W., Hommais, F., & Reverchon, S. (2019). APERO: A genome-wide approach for identifying bacterial small RNAs from RNA-Seq data. *Nucleic Acids Research*, *47*, e88–e88.

Li, J., Ma, W., Zeng, P., Wang, J., Geng, B., Yang, J., & Cui, Q. (2015). LncTar: A tool for predicting the RNA targets of long noncoding RNAs. *Briefings in bioinformatics*, *16*, 806–812.

Li, Z. T., Zhang, R. L., Bi, X. G., Xu, L., Fan, M., Xie, D., Xian, Y., Wang, Y., Li, X. J., Wu, Z. D., & Zhang, K. X. (2015). Outer membrane vesicles isolated from two clinical Acinetobacter baumannii strains exhibit different toxicity and proteome characteristics. *Microbial Pathogenesis*, *81*, 46–52.

Liu, Q., Yi, J., Liang, K., Zhang, X., & Liu, Q. (2017). Outer membrane vesicles derived from salmonella enteritidis protect against the virulent wild-type strain infection in a mouse model. *Journal of Microbiology and Biotechnology*, *27*, 1519–1528.

Mader, U., Nicolas, P., Depke, M., Pane-Farre, J., Debarbouille, M., van der Kooi-Pol, M. M., Guerin, C., Derozier, S., Hiron, A., Jarmer, H., Leduc, A., Michalik, S., Reilman, E., Schaffer, M., Schmidt, F., Bessieres, P., Noirot, P., Hecker, M., Msadek, T., … van Dijl, J. M. (2016). Staphylococcus aureus transcriptome architecture: From laboratory to infection-mimicking conditions. *Plos Genetics*, *12*, e1005962.

Madetoja, J., Hänninen, M.-L., Dalsgaard, V. H.-K. I., & Wiklund, T. (2001). Phenotypic and genotypic characterization of Flavobacterium psychrophilum from Finnish fish farms, *Journal of Fish Diseases*, 469–479.

Makino, T., Mizawa, M., Yoshihisa, Y., Yamamoto, S., Tabuchi, Y., Miyai, M., Hibino, T., Sasahara, M., & Shimizu, T. (2020). Trichohyalin-like 1 protein plays a crucial role in proliferation and anti-apoptosis of normal human keratinocytes and squamous cell carcinoma cells. *Cell Death Discovery*, *6*, 109.

Mann, M., Wright, P. R., & Backofen, R. (2017). IntaRNA 2.0: Enhanced and customizable prediction of RNA-RNA interactions. *Nucleic Acids Research*, *45*, W435–w439.

Marancik, D., Gao, G., Paneru, B., Ma, H., Hernandez, A. G., Salem, M., Yao, J., Palti, Y., & Wiens, G. D. (2014). Whole-body transcriptome of selectively bred, resistant-, control-, and susceptible-line rainbow trout following experimental challenge with Flavobacterium psychrophilum. *Frontiers in Genetics*, *5*, 453.

Marshansky, V., & Futai, M. (2008). The V-type H+-ATPase in vesicular trafficking: Targeting, regulation and function. *Current Opinion in Cell Biology*, *20*, 415–426.

Mendoza, J. F., Cáceres, J. R., Santiago, E., Mora, L. M., Sánchez, L., Corona, T. M., Machuca, C., Zambrano, I. R., Martínez, R. D., & Weiss-Steider, B. (1990). Evidence that G-CSF is a fibroblast growth factor that induces granulocytes to increase phagocytosis and to present a mature morphology, and that macrophages secrete 45-kd molecules with these activities as well as with G-CSF-like activity. *Experimental Hematology*, *18*, 903–910.

Moller, J. D., Barnes, A. C., Dalsgaard, I., & Ellis, A. E. (2005). Characterisation of surface blebbing and membrane vesicles produced by Flavobacterium psychrophilum. *Diseases of Aquatic Organisms*, *64*, 201–209.

Nematollahi, A., Decostere, A., Pasmans, F., & Haesebrouck, F. (2003). Flavobacterium psychrophilum infections in salmonid fish. *Journal of Fish Diseases*, *26*, 563–574.

Oliver, C., Valenzuela, K., Hernandez, M., Sandoval, R., Haro, R. E., Avendano-Herrera, R., Carcamo, J. G., Villar, M. T., Artigues, A., Garduno, R., & Yanez, A. J. (2016). Characterization and pathogenic role of outer membrane vesicles produced by the fish pathogen Piscirickettsia salmonis under in vitro conditions. *Veterinary Microbiology*, *184*, 94–101.

Padalon-Brauch, G., Hershberg, R., Elgrably-Weiss, M., Baruch, K., Rosenshine, I., Margalit, H., & Altuvia, S. (2008). Small RNAs encoded within genetic islands of Salmonella typhimurium show host-induced expression and role in virulence. *Nucleic Acids Research*, *36*, 1913–1927.

Pandiripally, V., Wei, L., Skerka, C., Zipfel, P. F., & Cue, D. (2003). Recruitment of complement factor H-like protein 1 promotes intracellular invasion by group A streptococci. *Infection and Immunity*, *71*, 7119–7128.

Paneru, B., Ali, A., Al-Tobasei, R., Kenney, B., & Salem, M. (2018). Crosstalk among lncRNAs, microRNAs and mRNAs in the muscle 'degradome' of rainbow trout. *Scientific Reports*, *8*, 8416.

Paneru, B., Al-Tobasei, R., Palti, Y., Wiens, G. D., & Salem, M. (2016). Differential expression of long non-coding RNAs in three genetic lines of rainbow trout in response to infection with Flavobacterium psychrophilum. *Scientific Reports*, *6*, 36032.

Papenfort, K., & Bassler, B. L. (2016). Quorum sensing signal-response systems in Gram-negative bacteria. *Nature Reviews Microbiology*, *14*, 576–588.

Queval, C. J., Song, O. R., Carralot, J. P., Saliou, J. M., Bongiovanni, A., Deloison, G., Deboosere, N., Jouny, S., Iantomasi, R., Delorme, V., Debrie, A. S., Park, S. J., Gouveia, J. C., Tomavo, S., Brosch, R., Yoshimura, A., Yeramian, E., & Brodin, P. (2017). Mycobacterium tuberculosis controls phagosomal acidification by targeting CISH-mediated signaling. *Cell Reports*, *20*, 3188–3198.

Quinlan, A. R., & Hall, I. M. (2010). BEDTools: A flexible suite of utilities for comparing genomic features. *Bioinformatics*, *26*, 841–842.

Renelli, M., Matias, V., Lo, R. Y., & Beveridge, T. J. (2004). DNA-containing membrane vesicles of Pseudomonas aeruginosa PAO1 and their genetic transformation potential. *Microbiology (N Y Reading)*, *150*, 2161–2169.

Schmittgen, T. D., & Livak, K. J. (2008). Analyzing real-time PCR data by the comparative C(T) method. *Nature Protocols*, *3*, 1101–1108.

Semple, S. L., Bols, N. C., Lumsden, J. S., & Dixon, B. (2020). Understanding the pathogenesis of Flavobacterium psychrophilum using the rainbow trout monocyte/macrophage-like cell line, RTS11, as an infection model. *Microbial Pathogenesis*, *139*, 103910.

Sharma, L., Feng, J., Britto, C. J., & Dela Cruz, C. S. (2020). Mechanisms of epithelial immunity evasion by respiratory bacterial pathogens. *Frontiers in Immunology*, *11*, 91.

Silverstein, J. T., Vallejo, R. L., Palti, Y., Leeds, T. D., Rexroad, C. E., 3rd, Welch, T. J., Wiens, G. D., & Ducrocq, V. (2009). Rainbow trout resistance to bacterial cold-water disease is moderately heritable and is not adversely correlated with growth. *Journal of Animal Science*, *87*, 860–867.

Sjostrom, A. E., Sandblad, L., Uhlin, B. E., & Wai, S. N. (2015). Membrane vesicle-mediated release of bacterial RNA. *Scientific Reports*, *5*, 15329.

Soares-Silva, M., Diniz, F. F., Gomes, G. N., & Bahia, D. (2016). The mitogen-activated protein kinase (MAPK) pathway: Role in immune evasion by trypanosomatids. *Frontiers in Microbiology*, *7*, 183.

Starliper, C. E. (2011). Bacterial coldwater disease of fishes caused by Flavobacterium psychrophilum. *Journal of Advanced Research*, *2*, 97–108.

Sundell, K., Landor, L., Nicolas, P., Jorgensen, J., Castillo, D., Middelboe, M., Dalsgaard, I., Donati, V. L., Madsen, L., & Wiklund, T. (2019). Phenotypic and genetic predictors of pathogenicity and virulence in Flavobacterium psychrophilum. *Frontiers in Microbiology*, *10*, 1711.

Takayama, S., Reed, J. C., & Homma, S. (2003). Heat-shock proteins as regulators of apoptosis. *Oncogene*, *22*, 9041–9047.

Turnbull, L., Toyofuku, M., Hynen, A. L., Kurosawa, M., Pessi, G., Petty, N. K., Osvath, S. R., Carcamo-Oyarce, G., Gloag, E. S., Shimoni, R., Omasits, U., Ito, S., Yap, X., Monahan, L. G., Cavaliere, R., Ahrens, C. H., Charles, I. G., Nomura, N., Eberl, L., & Whitchurch, C. B. (2016). Explosive cell lysis as a mechanism for the biogenesis of bacterial membrane vesicles and biofilms. *Nature Communications*, *7*, 11220.

Uribe-Querol, E., & Rosales, C. (2020). Phagocytosis: Our current understanding of a universal biological process. *Frontiers in Immunology*, *11*, 1066.

van den Boorn, J. G., Dassler, J., Coch, C., Schlee, M., & Hartmann, G. (2013). Exosomes as nucleic acid nanocarriers. *Advanced Drug Delivery Reviews*, *65*, 331–335.

van der Pol, L., Stork, M., & van der Ley, P. (2015). Outer membrane vesicles as platform vaccine technology. *Biotechnology Journal*, *10*, 1689–1706.

Wang, J., Rennie, W., Liu, C., Carmack, C. S., Prevost, K., Caron, M. P., Masse, E., Ding, Y., & Wade, J. T. (2015). Identification of bacterial sRNA regulatory targets using ribosome profiling. *Nucleic Acids Research*, *43*, 10308–10320.

Westermann, A. J., Forstner, K. U., Amman, F., Barquist, L., Chao, Y., Schulte, L. N., Muller, L., Reinhardt, R., Stadler, P. F., & Vogel, J. (2016). Dual RNA-seq unveils noncoding RNA functions in host-pathogen interactions. *Nature*, *529*, 496–501.

Wiens, G. D., LaPatra, S. E., Welch, T. J., Evenhuis, J. P., Rexroad, C. E. III., & Leeds, T. D (2013). On-farm performance of rainbow trout (Oncorhynchus mykiss) selectively bred for resistance to bacterial cold water disease: Effect of rearing environment on survival phenotype. *Aquaculture*, *388*, 128–136.

SUPPORTING INFORMATION

Additional supporting information can be found online in the Supporting Information section at the end of this article.

How to cite this article: Chapagain, P., Ali, A., Kidane, D. T., Farone, M., & Salem, M. (2024). Characterisation of sRNAs enriched in outer membrane vesicles of pathogenic *Flavobacterium psychrophilum* causing Bacterial Cold Water Disease in rainbow trout. *Journal of Extracellular Biology*, *3*, e161. https://doi.org/10.1002/jex2.161